REVIEW ARTICLE

Review of radiation damage in GaN-based materials and devices

Stephen J. Pearton[a] and Richard Deist
Department of Materials Science and Engineering, University of Florida, Gainesville, Florida 32606

Fan Ren and Lu Liu
Department of Chemical Engineering, University of Florida, Gainesville, Florida 32611

Alexander Y. Polyakov
Institute of Rare Metals, Moscow, 119017, B. Tolmachevsky, 5, Russia

Jihyun Kim
Department of Chemical and Biological Engineering, Korea University, Anam-dong, Sungbuk-gu, Seoul, 136-713, Korea

(Received 10 January 2013; accepted 18 March 2013; published 9 April 2013)

A review of the effects of proton, neutron, γ-ray, and electron irradiation on GaN materials and devices is presented. Neutron irradiation tends to create disordered regions in the GaN, while the damage from the other forms of radiation is more typically point defects. In all cases, the damaged region contains carrier traps that reduce the mobility and conductivity of the GaN and at high enough doses, a significant degradation of device performance. GaN is several orders of magnitude more resistant to radiation damage than GaAs of similar doping concentrations. In terms of heterostructures, preliminary data suggests that the radiation hardness decreases in the order AlN/GaN > AlGaN/GaN > InAlN/GaN, consistent with the average bond strengths in the Al-based materials. © *2013 American Vacuum Society*. [http://dx.doi.org/10.1116/1.4799504]

I. INTRODUCTION

The GaInAlN materials system has a number of prominent device applications in UV and visible lighting, full color displays, and high voltage electronics. Nitride-based light-emitting diodes (LEDs) and laser diodes (LDs) are the main semiconductor light sources for the UV-blue regions and are commonly employed in applications such as traffic lights, white light illumination, and data storage. In addition, AlGaN/GaN photodetectors are effective in solar-blind UV detection. More recently, the use of nitride-based electronic devices has attracted interest. AlGaN/GaN and InAlN/GaN high electron mobility transistors (HEMTs) and GaN or AlGaN Schottky diodes show promise for high power switching applications. In particular, some of the applications are in military or commercial systems, such as satellites or avionics, where radiation hardness is a key requirement.[1–33] In space-based applications, electronic systems are exposed to fluxes of protons, α-particles, and heavier ions. Additional sources of radiation include the van Allen belts, with high proton and electron fluxes and the Sun, which produces both protons and heavier ions with variable composition during solar flares. Finally, primary cosmic rays create secondary cascades of protons, neutrons, mesons, and nuclear fragments whose intensity is a maximum at 18 km and decreases with distance down to sea level. At normal aircraft cruising altitudes, the radiation flux encountered is several hundred times the ground level intensity.

In this paper, we summarize the current state-of-the-art for radiation damage studies in GaN materials and devices. Most of the work has focused on the effect of protons, neutrons, and electrons and less has been published on gamma and x-rays. Degradation in material properties and device performance is mainly due to carrier trapping and mobility reduction by radiation damage. The use of controlled doses of radiation also provides a method for introducing point defects and more extended disordered regions for basic defect science studies.

II. THRESHOLD DISPLACEMENT ENERGY: THEORY AND EXPERIMENT

The initial measurements of displacement threshold energy for GaN (Ref. 5) consisted of monitoring changes in luminescence spectra of GaN LEDs as a function of electron irradiation energies in the range of 300–1400 keV. Generation of the band attributed to the formation of Ga vacancies started at an electron energy of 440 keV, corresponding to a Ga displacement energy of 19 eV. In a comparison of defect production between 2 MeV protons and 2.5 MeV electrons, the protons were 1000 times more effective in displacing atoms, whereas calculations of the number of displaced atoms based on the measured threshold energy predicted a ratio of 250. The discrepancy was attributed to the difference in defect self-annealing rates, which depend on irradiating particle type and energy. The measured displacement threshold in GaN was higher than in Si and GaAs, and close to that in SiC, but lower than in diamond. This

[a]Electronic mail: spear@mse.ufl.edu

trend reflects the difference in the bond strength of the respective materials and can serve as an indication of relative radiation hardness. Measurements of the changes in electrical properties of undoped n-GaN films irradiated with electrons with energies 700–1000 keV showed that nitrogen vacancies were introduced with a rate of $\sim 1\,cm^{-1}$.[8] Molecular dynamics calculations of displacement effects in GaN explained why discrepancies could exist when comparing effectiveness of the introduction of radiation defects by various particles based on the values of threshold defect formation.[21] Some of the conclusions included existence of a wide distribution of threshold energies for both Ga and N sublattices and that the effects of recombination induced by self-annealing caused by athermal local energy transfer are important. This study found minimal energies of defect formation of 18 eV for Ga and 22 eV for nitrogen. The average displacement energies were much higher, 45 eV for Ga and 109 eV for N.

Additional insight can be gained from high energy ion implantation studies.[24] Experimental measurements of defect accumulation produced by ion implantation at different temperatures showed radiation defects in GaN were mobile even at low temperatures, and doses of ions producing amorphization were more than an order of magnitude higher than for GaAs.[24] For hydrogen irradiation at doses exceeding $\sim 10^{16}\,cm^{-2}$, formation of hydrogen bubbles occurred. For heavy ions (starting with Si), the main factor in defect production was ion mass and energy and the number of primary displacements initiated. Recombination of radiation defects during irradiation was prominent even at low temperature and the rate of recombination increased with temperature.[24] At room temperature, the doses of radiation producing amorphization increased from $10^{14}\,cm^{-2}$ for heavy ions to $\sim 10^{16}\,cm^{-2}$ for light ions, but increasing the implantation temperature increased the amorphization threshold by several orders of magnitude. For heavily amorphized material, the formation of N_2 bubbles was observed.

A. Energy levels of radiation defects in GaN

It is expected that ionizing radiation such as electrons and protons will produce point defects and complexes thereof.[35–52] The primary defects produced in GaN by irradiation are Frenkel pairs in the Ga and N sublattices.[53–63] The theory of N vacancies in $Al_xGa_{1-x}N$ suggests that these are shallow donors in GaN,[26] but in AlN, this same defect is a deep trap. The A_1 or s-like deep level lies slightly below the conduction-band minimum of GaN, while its T_2 level lies above the conduction-band edge. The A_1 level of the neutral defect contains two electrons. The nitrogen vacancies in GaN are electronic resonances with levels in the conduction band. By capturing electrons, they are turned into effective-mass-like (EM) shallow donors[26] Experimental measurements indicate that these N vacancies have ionization energies of 40–60 meV in GaN.[2] For nitrogen interstitials, Ni, theoretical calculations predict the existence of a deep acceptor near 1 eV from the conduction band edge.[35,36] The same theoretical studies indicate that the Ga vacancy has a fully occupied s-like A_1 level just below the valence-band edge and a half-occupied p-like T_2 level above but near the valence-band edge.[26] Hence, the Ga vacancies are traps for both holes and electrons, tending to make GaN semi-insulating. Ga vacancies in the doubly charged state produce an acceptor state near Ev+1 eV, while Ga interstitials form negative-U type donors whose +/0 transition level is close to the conduction band edge and the $3^+/2^+$ charge transition level is located near Ev+2.6 eV (Ec−0.8 eV).[35,36]

Look *et al.*[8] showed that electron irradiation with energies 0.7–1 MeV introduced new donors with ionization energy close to 0.06 eV with introduction rate of $1\,cm^{-1}$. The net electron concentration hardly changed while the mobility of electrons decreased with increasing dose. Analysis of the temperature dependence of mobility suggested that acceptor centers were introduced at a rate similar to the rate of the 0.06 eV donors. The observed effects were explained by the formation of Frenkel pairs in the nitrogen sublattice, with the nitrogen vacancies V_N responsible for the 0.06 eV donors and nitrogen interstitials N_i associated with the compensating acceptors. Deep level transient spectroscopy (DLTS) performed on 1 MeV electron irradiated n-GaN showed deep electron traps with activation energy 0.9 eV attributed to N_i acceptors.[29] GaN irradiated with ^{60}Co γ-rays also showed electron traps with activation energy of 80 meV.[6] This ionization energy is close to that reported for V_N donors.[8] In undoped n-GaN irradiated with 10 MeV electrons, deep acceptor traps with activation energy 1 eV were attributed to N_i acceptors.[2] 2.5 MeV electron irradiation at 4.2 K produced a strong defect photoluminescence PL band centered at 0.95 eV.[64] This PL line was attributed to the Ga vacancy, V_{Ga}, with a level at E_v+1 eV.

A consideration of carrier removal rates and corresponding defect introduction rates can shed light on the types of defects produced in GaN by radiation. If the only defects created were Frenkel pairs, then at low doses, the carrier removal rate for n-GaN while the density of radiation defects is lower than the concentration of dopant donors would be equal to the production rate of V_{Ga} and N_i. Similarly, at high irradiation doses the Fermi level in the GaN would be pinned at whichever of the two EM-like native donors, V_N or V_{Ga}^{1+} was shallower in ionization energy. In an analogous fashion, in p-type GaN, the initial carrier removal rate should be close to that in n-type until the total density of V_N and Ga_i donors exceeds the density of acceptor dopants. Once that occurs, the Fermi level should become pinned at the V_{Ga} level near E_v+1 eV. This simple picture does not take account of recombination of primary defects or formation of defect complexes involving dopants or other defects. The radiation-induced defects may also complex with heavily disordered regions typical of those formed by neutron irradiation.

GaN irradiated with electrons, γ-rays and protons with energies in the mega-electron-volt range show a common set of electron traps with electrical activation energies 0.13 eV, 0.16 eV, and 0.18–0.2 eV.[6,29–31,50–53] The latter traps show a spread in ionization energies and produce a broad feature in DLTS due to the proximity of emission rates of components, but this can be deconvoluted into separate defect

contributions due to the difference in electron capture cross sections.[6,29–31,47] For the 0.18–0.20 eV traps, the activation energy is the sum of the trap ionization energy, which is 0.06 eV, and the capture activation energy of about 0.14 eV.[29] These traps are likely complexes of nitrogen vacancies with other native defects, such as nitrogen interstitials or antisite defects.[29] The shallower defects are also believed to be V_N-related.[11] The 0.13 and 0.18–0.2 eV electron traps are expected to be donor-like.[29] In this case, the carrier removal in irradiated n-GaN should then be regulated by the balance between relatively shallow V_N-related donors, deep N_i acceptors, deep Ga_i donors, and V_{Ga} acceptors. However, this simplified picture does not agree with the dependence of 0.10–0.20 eV trap ionization energy dependence on applied electric field, which shows these traps are acceptors.[15] An alternative identity of these traps suggests they may be $V_{Ga}N_i^{2-}$ complexes.[30,31,47] DLTS spectra of n-GaN films irradiated with light particles are dominated by these shallow electron traps. Only in particular circumstances, such as for much higher electron energies,[2] heavier ions like He or N,[30,46] for neutron irradiation,[51] or higher doses in proton implanted samples [150 keV protons with dose over $5 \times 10^{14}\,cm^{-2}$ (Refs. 2 and 53)], are deeper traps commonly detected. Electron traps that are generally observed in these higher dose or heavier ion cases show activation energies of 0.75–0.8 eV and 0.95–1.2 eV.[2,31,65–68] The 0.8 eV traps show a decrease of the ionization energy with increasing electric field whereas the 1 eV traps energy does not vary with electric field. The decrease in ionization energy with electric field is expected for donors because of the Poole–Frenkel effect, while the invariance of ionization energy with field is characteristic of acceptors that are neutral when they emit an electron.[2] Theoretical calculations have identified the deep donors as due to Ga_i^{2+} and the acceptors to N_i^{2+}.[2,29,31,47,54]

Implantation of n-GaN with 150 keV protons to doses higher than $5 \times 10^{14}\,cm^{-2}$ also created deep electron traps with ionization energies that increased from 0.2 eV at low dose to 0.25, 0.32, and 0.45 eV at progressively higher dose. This behavior could be explained by formation of larger complexes through addition of new radiation defects to the more simple radiation defects formed at low doses.[2,55] Studies of neutron transmutation doped n-GaN (Ref. 55) indicate that the 0.2 and 0.45 eV traps incorporate donors.

The understanding of hole traps in irradiated GaN is far less complete compared to electron traps. Part of the difficulty is simply accessing these minority carrier traps. For proton irradiation, deep electron traps near Ec−0.5–0.6 eV and deep hole traps with levels near Ev+0.3 eV and Ev+0.85 eV were introduced.[65,66] The electron traps at Ec−0.5–0.6 eV are believed to be complexes of Mg acceptors with native defects and were shown to also give rise to intense blue defect luminescence band centered at 2.9 eV.[33,34] The Ev+0.85 eV traps are probably the same as the V_{Ga}-related hole traps in n-type films. Their in-grown concentration in p-type GaN should be very low because of the high formation energy,[35] but irradiation can introduce such defects and produce the yellow luminescence band in heavily irradiated p-GaN films despite the fact that the yellow luminescence might be absent in the nonirradiated p-GaN starting material.[65] A typical evolution of DLTS spectra of hole traps in electron irradiated n-GaN with dose is shown in Fig. 1.

Theory predicts the major acceptor defects in the lower half of the bandgap are related to V_{Ga} (triple acceptors, with the highest ionization level near E_v+1 eV) or V_{Ga} complexes with O (double acceptors with level near E_v+1.2 eV), with Si (E_v+1 eV) or with H (E_v+1 eV). Positron annihilation spectroscopy experiments show that irradiation mostly produces V_{Ga}-O complexes[5] while optically detected magnetic resonance data suggest production of mobile Ga_i.[28] In most of the metalorganic chemical vapor deposition (MOCVD) and epitaxially laterally overgrown (ELOG) n-GaN we have examined, the spectra are dominated by the so-called H1 hole traps with ionization energy of $E_v + 0.95$ eV associated with V_{Ga}-Si complexes. Electron and neutron irradiation of undoped and lightly Si doped ELOG and MOCVD n-GaN films invariably produces a decrease of apparent H1 concentration due to lower effective injection level and possibly due to recombination with mobile Ga_I. In more heavily doped samples, the H1 concentration first slightly increases due to formation of additional V_{Ga}-Si complexes and then decreases as in undoped films. Hole traps in the lower half of the bandgap of electron irradiated MOCVD and ELOG n-GaN play only a minor role in compensation.

To summarize the comparison between the radiation responses of n-and-p type GaN, in p-type material implanted

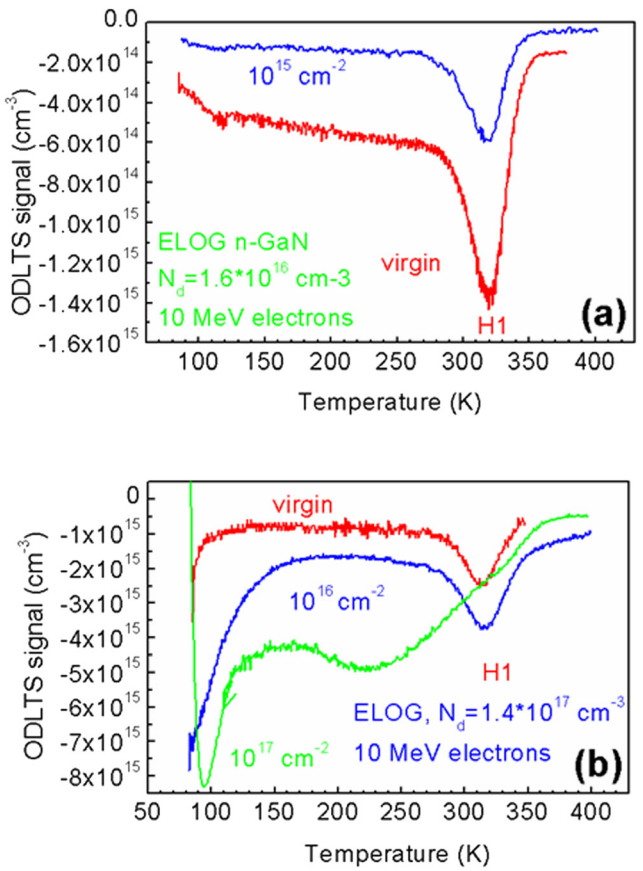

FIG. 1. (Color online) Hole trap spectra in ELOG n-GaN irradiated with different doses of 10 MeV electrons (a) dose of $1.6 \times 10^{16}\,cm^{-3}$ and (b) $1.4 \times 10^{17}\,cm^{-3}$.

with 100 keV protons, the degradation of luminescence intensity starts for doses of 10^{12} cm^{-2}. Decreases in hole concentration occurs for doses of 10^{13} cm^{-2}. Both threshold doses are more than an order of magnitude lower than in proton implanted n-GaN, probably because of efficient complex formation between the primary radiation defects and the Mg acceptors present in very high concentrations. Table I summarizes trap levels reported in irradiated GaN. The large number of levels suggests that impurities and extended defects are likely to interact with the primary radiation-induced defects.

B. Carrier removal rates and deep trap introduction rates; disordered regions

One of the fundamental aspects of the response of GaN to fluxes of radiation is the mechanism for the observed changes of electrical properties of irradiated material and the position of the Fermi level after high doses of radiation. The calculation of nonionizing energy loss (NIEL) for different types of radiation is a useful guide to how much displacement damage will be created.[58–62] NIEL is a calculation of the rate of energy loss due to atomic displacements as an incident

TABLE I. Defects introduced by various types of irradiation in GaN.

Material type, dopant concentration (cm^{-3})	Radiation type	Carrier removal rate, (cm^{-1})	Defect levels (activation energy (eV) from conduction C or valence V), defect type (donor D, acceptor A)	Defect production rate (cm^{-1})	Proposed identity	References
n-GaN, 10^{17}	^{60}Co γ-rays, 21 MRad	-	0,09, C,?	9.1	G1 = ER1	6
			0.11, C,?	7.3	G2 = ER2	
			0.14, C,?	4.8	G3 = ER3	
n-GaN, 10^{17}	0.7-1 MeV electrons	-	0.06, C, D	1	V_N	8
			?,?,A	1	N_i	
n-GaN,10^{17}	1 MeV electrons	-	0.13,C,D,	~0.1	ED1 = ER2	11 and 29
			0.2,C,D	~0.1	ED2 = ER3	
			0.9,C,?	~0.1	AD2 = Ni	
n-GaN, 10^{17}	1 MeV electrons	-	0.18, C, D	0.2	V_N-N_i	11 and 29
			0.06	1	V_N	11 and 29
n-GaN,10^{16}	10 MeV electrons	0.4	0.18, C, D	0.2	ED2 = ER3	2
			1, C, A	0.8	N_i	2
n-GaN, 10^{16}	0.2–2.5 MeV	-	0.13, C,?	-	ER1	31
			0.16, C,?	-	ER2	
			0.2,C, A	-	ER3 = $V_{Ga}N_i^{2-}$	
n-GaN,10^{16}	Protons, 2 MeV	260	0.13, C,?	30	ER1	31
			0.16, C,?	400	ER2	
			0.2, C, A	600	ER2	
n-GaN,10^{16}	Protons, 150 keV	100	0.2, C,?		ER3	65
			0.25, C,?		Complex of ER3	
			0.32, C,?		Complex of ER3	
			0.45, C,?		Complex of ER3	
			0.6,C,A			
			0.8, C, D		Ga_i	
n-GaN, 2×10^{18}	Protons, 150 keV	10 000				75
n-GaN, 4×10^{17}	Protons, 150 keV	3500				75
n-GaN, 10^{16}	5.4 MeV He	-	0.2,C,A	3300	ER3	31
			0.78, C, D	1500		
			0.95, C, A	3300	N_i	
n-GaN, 10^{16}	N ions, 300 keV	-	0.7, C,?			17
n-GaN, 10^{16},	Fast reactor neutrons	5	0.2, C, D		ER3	54
			0.8, C, D		Ga_i	
n-GaN, 1e^{17}	2 MeV electrons, 4.2 K		0.9, V, A		V_{Ga}	28
			0.8, C, D		Ga_i	
p-GaN, 2×10^{17} (MBE)	Fast reactor neutrons	100	0.5, C,?		Mg-related	66
			0.85, V, A		V_{Ga}	
			0.9, C,?		Between Ga_i and N_i	
p-GaN, 10^{18} (HVPE)	Fast reactor neutrons	100	0.5, C,?		Mg-related	66
			0.85, V, A		V_{Ga}	
			0.9, C,?		Between Ga_i and N_i	
p-GaN, 10^{18}	Protons, 100 keV	10 000	0.5, C,?		Mg-related	116
			0.3, V, A			
			0.85, V, A		V_{Ga}	

particle traverses a material. There are a number of transport codes for calculating this, including the Monte Carlo code stopping and range of ions in matter (SRIM).[58] This has traditionally been used to calculate projected ranges of ions implanted in semiconductors but also includes the stopping powers and nuclear energy loss for ions traversing a target material. The product of the NIEL and the particle fluence gives the displacement damage energy along the track.

As an example of how radiation damage degrades the electrical properties of GaN, Fig. 2 shows the carrier concentration (a) and mobility changes (b) for n-GaN samples irradiated with 10 MeV electrons as a function of dose. The carrier removal rate is 0.4 cm^{-1}, while the introduction rates for the 0.18 eV traps and the 1 eV traps are 0.2 cm^{-1} and 0.8 cm^{-1}, respectively. The contribution from the other acceptors, the V_{Ga}-related E_v+0.9 eV hole traps, is underestimated by the interference of the 1 eV electron traps due to N_i acceptors. The upper limit of the V_{Ga} introduction rate is ~0.4 cm^{-1}. If we assume that the initial carrier removal rate 0.4 cm^{-1} comes from the difference in introduction rates of all these acceptors and the introduction rate of the 0.06 eV V_N donors, the latter should be close to 1.4 cm^{-1}, i.e., ~7 times that of the 0.18 eV traps. A similar relation between

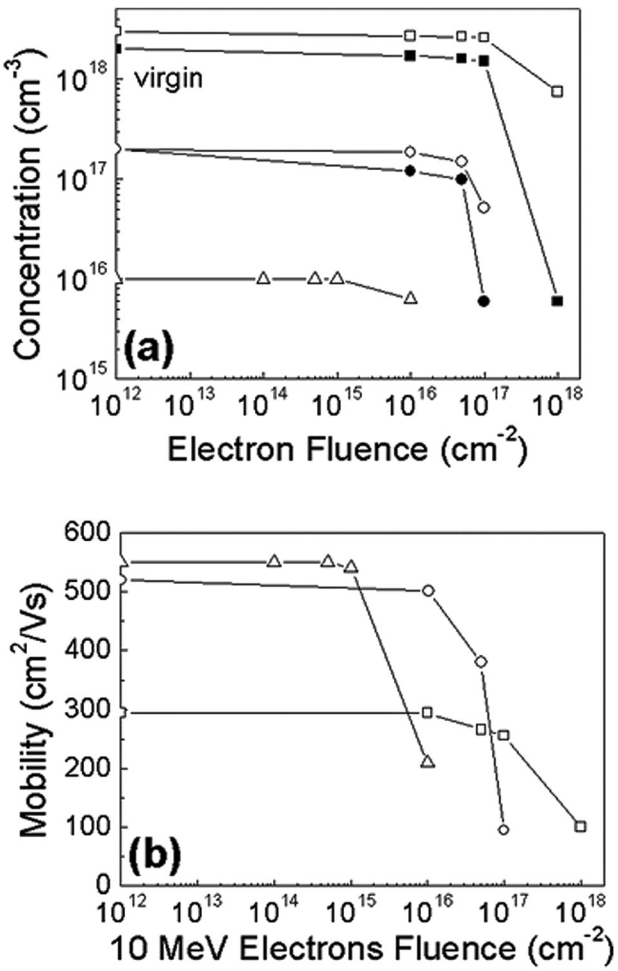

FIG. 2. Decrease in electron concentration (a) or electron mobility (b) in n-GaN films of different doping concentration irradiated with 10 MeV electrons to different doses. Reprinted with permission from J. Appl. Phys. **109**, 123703 (2011). Copyright 2011 American Institute of Physics.

the concentrations of these traps was determined from electron concentration and mobility fitting and DLTS measurements for n-GaN irradiated with 1 MeV electrons (1 cm^{-1} for the V_N centers versus 0.2 cm^{-1} for the 0.18 eV centers).[40] Hence, the data on electron removal by relatively low energy electrons can be explained by the introduction rates of well-documented radiation point defects. Similar conclusions hold for proton irradiation of GaN.

The situation for neutron irradiation of GaN is quite different because of the different types of damage created. Displacement defects in GaN produced by MeV neutrons are not randomly dispersed, but are clustered within the cascades of primary Ga and N recoils.[64–69] Schematics of the perfect GaN lattice and those containing both disordered regions typical of those created by neutrons and point defects typical of those created by protons and electrons are shown in Fig. 3. The main deep traps that can be associated with neutron irradiation are the 0.18 eV ER3 electron traps and the 0.8 eV Ga_I electron traps. However, the introduction rate of the shallower ER3 traps is much lower than for electron irradiation, the introduction rate of the 0.8 eV traps is below 1 cm^{-1} and is lower than the electron removal rate of 5 cm^{-1}. Since these traps are deep donors, they cannot contribute to carrier removal. The removal rate observed in neutron irradiated n-GaN might be explained by the formation of disordered regions disordered regions (DRs) first proposed for neutron irradiation of Si, now often referred to as Gossick regions.[70] In these regions, the bands are bent upwards by about 1 eV so that electrons released from deep centers inside these regions are swept out by the built-in electric field of the region and have to overcome the barrier of about 1 eV to be recaptured by their host traps. These Gossick-like DRs (Ref. 70) are heavily disordered core regions surrounded by the space charge region with a strong band bending. For high neutron irradiation doses, the outer regions of the DR's overlap and the Fermi level pinning position gives some idea of the Fermi level position in the core of the DR. Irrespective of the starting conductivity type and doping, the Fermi level is pinned near $E_c-(0.9–1)$ eV.[70] There is a correlation between this Fermi level pinning position and the pinning at the surface of n-GaN Schottky barriers, which is linked to the Fermi level stabilization F_s or charge neutrality concept introduced to explain similar correlations in many other III-V materials.[44,45] Several theoretical models have been offered to account for the observed F_s position in various materials. In one class of models, the Fermi level is believed to be trapped between the levels of the major native defects.[71,72] In GaN, it is located between the levels of N_I acceptors and of Ga_I donors. Lattice parameter measurements in heavily neutron irradiated GaN show an increase with dose, indicating that the dominant defects could be interstitials.[54,65,73–76] Rutherford backscattering experiments on neutron irradiated GaN also point to a very high density of interstitials, predominantly Ga_I.[74] In the other set of models, the F_s position is determined by the gap-induced states and can be estimated based on the known band structure.[73] Theoretical estimates from these models place the F_s in GaN near $E_c-0.8$ eV.[47]

Although any of these models qualitatively explain the behavior of neutron irradiated n- and p-GaN, a more

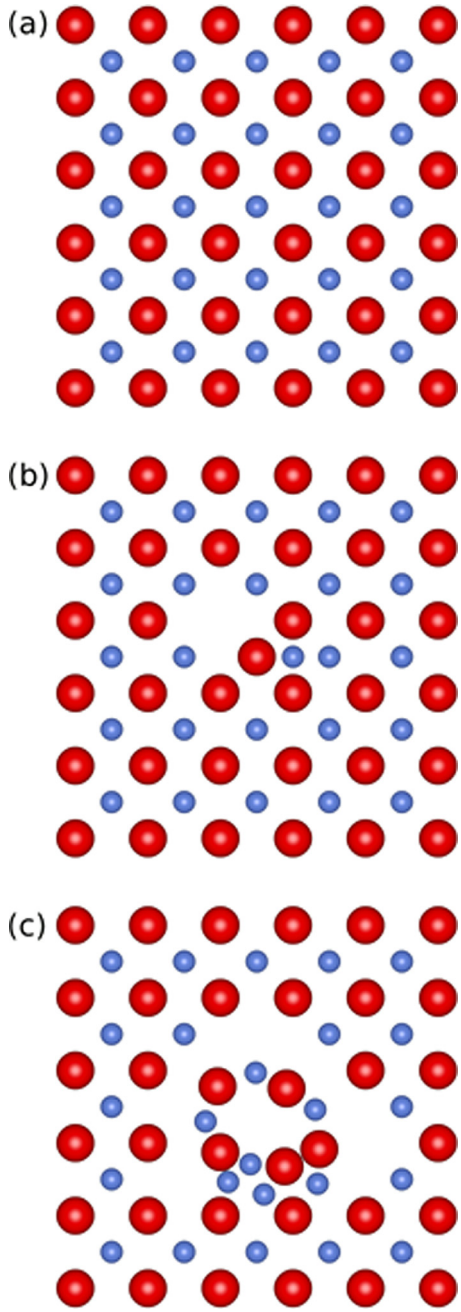

FIG. 3. (Color online) Schematic of (a) perfect GaN lattice prior to irradiation, (b) point defects created by ionizing radiation, and (c) Gossick zones typical of neutron irradiation.

quantitative model is still needed. The dependence of the carrier removal rate on starting donor density is not easily explained by the classical Gossick model. The carrier removal rate in neutron irradiated p-GaN is about 20 times higher than for n-GaN, despite the much higher concentration of acceptors in p-GaN than donors in n-GaN that should negate the effect of increased barrier height in p-GaN DRs.[64,65] The same asymmetry of carrier removal rates was observed for proton implanted p-GaN and n-GaN (Refs. 65, 77–81) and suggests that interaction of primary defects with Mg could be a factor in both cases.

Figure 4 summarizes the difference in carrier removal rates in n-GaN and AlGaN/GaN HEMTs for different doses

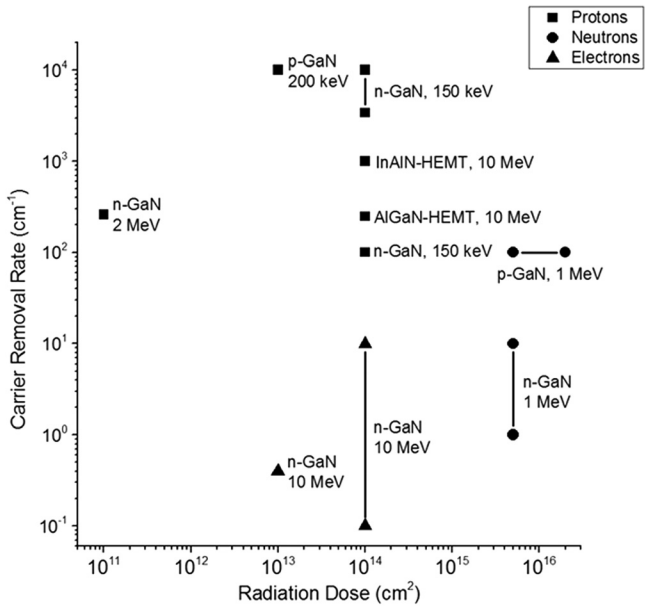

FIG. 4. Carrier removal rates in n-GaN films or AlGaN/GaN heterostructures as a function of dose for different types of radiation.

of common radiation species. Protons create more traps than electron irradiation of the same dose. Moreover, the initial data shown in Fig. 5 show that for the same proton dose, InAlN/GaN heterostructures suffer more degradation than their AlGaN/GaN counterparts. This is consistent with the average bond strengths in the Al-based materials.

C. Effect of irradiation on lifetime of nonequilibrium charge carriers

It is a common practice to characterize the effect of radiation damage on carrier lifetime by the lifetime degradation constant K_τ (Ref. 82)

$$I_o/I = 1 + K_\tau F, \tag{1}$$

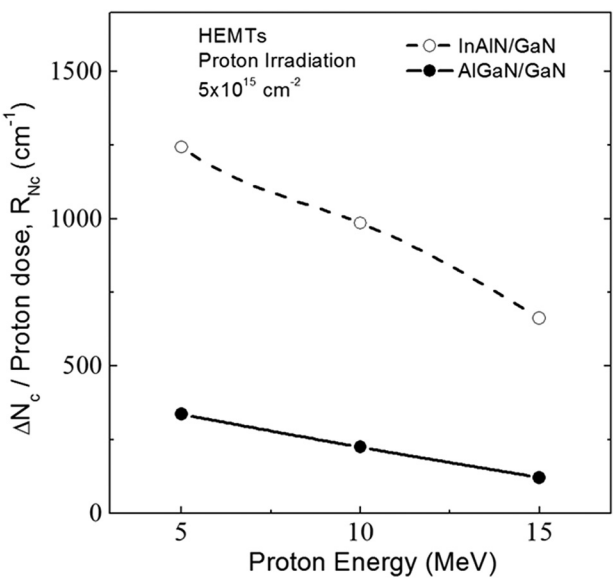

FIG. 5. Carrier removal rates by protons in InAlN/GaN and AlGaN/GaN HEMTs.

where I_o is the lifetime value before irradiation, and I is the lifetime after irradiation with the fluence F. Direct measurements of lifetimes in GaN are scarce. Proton irradiation with 150 keV protons at a dose $5 \times 10^{14}\,cm^{-2}$ decreased the diffusion length from 1.2 to 0.6 μm. From Eq. (1), the lifetime degradation coefficient K_τ (protons) is $\sim 1.6 \times 10^{-14}\,cm^2$ for such irradiation. For proton implanted n-GaN, there is a strong decrease in the measured lifetime and in bandedge luminescence intensity after doses at which deep electron traps 0.8 eV presumably associated with Ga_I were introduced.[2] In GaN, where the dislocation density is high, one has to consider possible effects of dislocations on diffusion length or lifetime.

D. Effects of dislocation density

GaN is mainly grown on lattice mismatched substrates and contains a high density of dislocations.[83–99] In standard GaN/sapphire structures, the dislocation density is $\sim 10^9\,cm^{-2}$, while optimization reduces this to $\sim 10^8\,cm^{-2}$. The dislocation density can be decreased to $\sim 10^6\,cm^{-2}$ for ELOG GaN. A schematic of the ELOG process is shown in Fig. 6. Thick (over 200 μm) GaN films grown on sapphire by hydride vapor phase epitaxy (HVPE) have typical dislocation densities below $10^7\,cm^{-2}$, as determined by etch pit counting or electron microscopy. Interaction of radiation defects with dislocations may need consideration for structures prepared by conventional epitaxy, which will have dislocation densities higher than for homoepitaxy or ELOG films. Advanced devices, such as high-power LEDs and LDs tend to be grown either on low-dislocation-density GaN substrates or using some version of the ELOG technique. This could have an impact on the type of radiation defects created in GaN-based devices.

The most understood manifestation of dislocations is the effect of spatial correlation of electron capture by deep traps decorating dislocations. This correlated capture has been

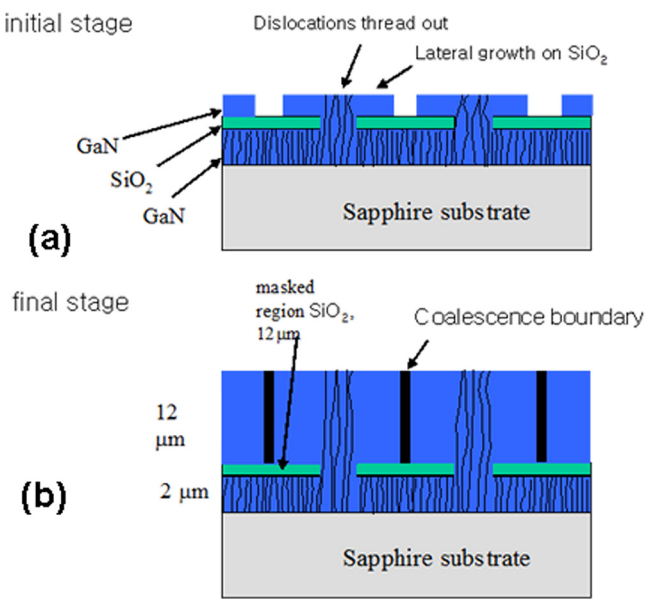

FIG. 6. (Color online) Schematic of initial stage (a) and final stage (b) of growth and dislocation propagation in ELOG GaN.

treated theoretically and experimentally.[100,101] The most obvious effect is the logarithmic dependence of the DLTS peak amplitude of the trap on the injection pulse length t_p. Such behavior has been reported for the 1 eV N_I-related acceptors and 0.78 and 0.95 eV electron traps introduced by 2 MeV proton irradiation.[31] These traps are possibly due to Ga_I deep donors and N_I deep acceptors. During irradiation, at least part of the interstitial defects can travel to dislocation boundaries and decorate them. Another factor is the impact of dislocations on mobility of charge carriers.[7,8,29] The theory predicts a strong increase of the electron mobility with decreasing dislocation density and increasing electron concentration, the latter due to enhanced screening of dislocations. However, the effect of dislocations on the carrier mobility is not reduced to the sum of contributions from individual dislocations. For dislocation densities exceeding $\sim 10^8\,cm^{-2}$ in GaN, dislocations form a cellular structure with dislocation boundaries formed mostly by the threading edge dislocations and characteristic grain size determined by the dislocation density. For carriers to travel over the grain boundaries involves overcoming a high potential barrier. When the electron concentration is high, tunneling through the barriers is efficient, and the material behaves as though electrical nonuniformities were not present. With increased doses of radiation, the electron concentration within the grains becomes lower and the potential barriers at the grains gain higher importance. For p-GaN, tunneling of holes is difficult even at high acceptor densities and hole mobility seldom shows "theoretical" temperature or concentration dependence.[2]

The cellular structure of GaN with high dislocation density has a profound effect on diffusion length of nonequilibrium carriers. The diffusion length in n-GaN in many cases is determined by the distance between the low-angle dislocation boundaries and hence by the dislocation density,[2] but the model is not valid for low-dislocation densities where the dislocations are randomly distributed and the diffusion length and the lifetime of charge carriers are determined mostly by defects other than dislocations.

For undoped n-GaN ELOG films with typical layer thickness of 12 μm, the residual donor concentration is generally much higher in the ELOG window region (dislocation density $\sim 10^8\,cm^{-2}$) than in the low dislocation density ($10^6\,cm^{-2}$) ELOG wing region ($\sim 10^{15}\,cm^{-3}$ vs $\sim 3 \times 10^{14}\,cm^{-3}$). In addition, the deep trap density in the ELOG wing region is usually about an order of magnitude lower than for standard MOCVD material, and the diffusion length in the low-dislocation-density ELOG wing is around 0.3 vs 0.17 μm in the high-dislocation-density window (the lifetime difference of 0.4 vs 0.1 ns). All of these factors lead to a typical band-edge emission intensity about five times higher in the ELOG windows.[52,59–61]

Neutron irradiation of undoped ELOG GaN resulted in a much lower effective removal rate than for standard MOCVD material, 1 vs $5\,cm^{-1}$, as shown in Fig. 7.[78] The 0.5–0.6 eV pseudo-hole-trap band in optical deep level transient spectroscopy of irradiated samples comes from persistent photoconductivity due to disordered regions. The Fermi

level position in heavily irradiated material is also the same, suggesting that no changes in the structure of the core regions of DRs occur with changing the dislocation density.

For MOCVD n-GaN, the carrier removal rate increases sublinearly (approximately as the square root of starting concentration) for concentrations below $2 \times 10^{16}\,\mathrm{cm}^{-3}$ and then, for higher concentrations, it levels off. For ELOG samples, the sublinear region extends to a higher starting donor doping of $1.35 \times 10^{17}\,\mathrm{cm}^{-3}$, the carrier removal rates at low concentrations are substantially lower than for MOCVD samples with similar concentration and the difference between MOCVD and ELOG films becomes less pronounced for higher donor densities. Figure 7 also shows the data for two bulk HVPE samples. These samples were irradiated with neutron fluences of $5 \times 10^{15}\,\mathrm{cm}^{-2}$ and $2 \times 10^{16}\,\mathrm{cm}^{-2}$. The first dose led to a decrease in the uncompensated donor concentration, as determined by C-V measurements. The points in Fig. 7 were derived from these measurements. After irradiation with the second dose of $2 \times 10^{16}\,\mathrm{cm}^{-2}$, both samples became highly resistive. The HVPE results lie considerably lower than the MOCVD or ELOG results and that the dependence of the removal rate on starting concentration is stronger. It is not clear why the carrier removal rates differ so much for the ELOG and bulk HVPE samples. This is not a consequence of dislocation density changes, because the dislocation density in the low-dislocation-density wing of ELOG samples is similar to the dislocation density in bulk HVPE samples. More likely, this has to do with the uniformity of dislocation distribution. For MOCVD GaN, the dislocations form a clear cellular pattern, with the typical size of dislocation cell of 0.3–0.5 μm. In ELOG GaN, wing regions with randomly distributed dislocations with density $\sim 5 \times 10^{6}\,\mathrm{cm}^{-2}$ are adjacent to the high dislocation-density window regions, whereas in HVPE samples, the dislocation density is uniformly low at $\sim 10^{7}\,\mathrm{cm}^{-2}$. This could be important for the probability of primary radiation defects to escape to the dislocations. It is well known that Ga vacancies (V_{Ga}) and Ga interstitials (Ga_i) are mobile at room temperature in GaN.[24] We also note that it has been discovered by electron beam induced current (EBIC) profiling in neutron irradiated ELOG n-GaN that the decrease of the charge collection efficiency in EBIC occurs much more rapidly in the parts of ELOG wing region close to the window region than in the bulk of the ELOG wing where the radiation induced changes are the lowest, as shown in Fig. 8. Typical DLTS spectra of electron and hole traps in the ELOG region are shown in Fig. 9—there are more hole traps created under these conditions.

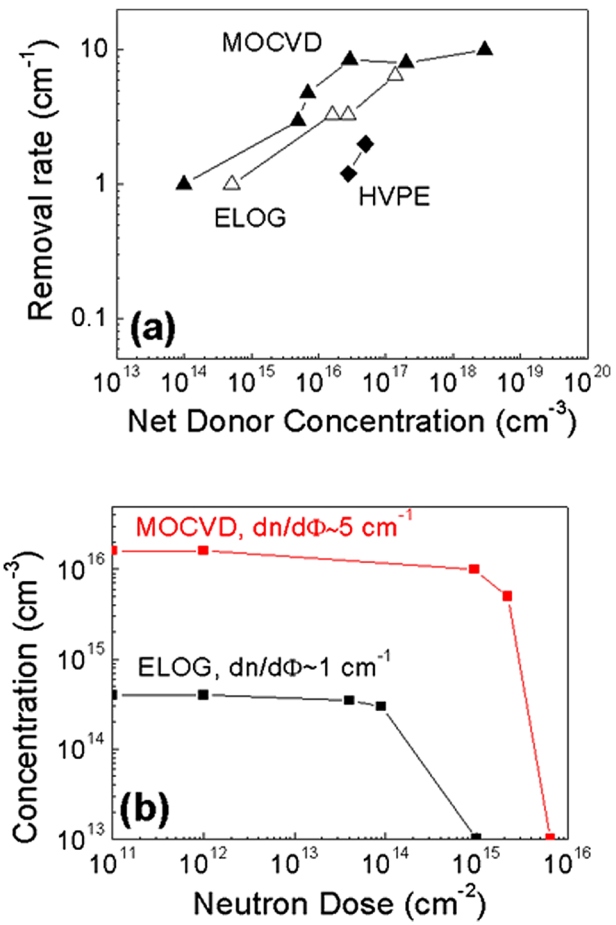

FIG. 7. (Color online) (a) Carrier removal rates for neutron irradiated MOCVD (solid triangles) and ELOG n-GaN (open triangles) samples with various donor doping; also shown are carrier removal rates for two bulk HVPE samples (solid diamonds). (b) Decrease in carrier concentration in n-GaN films grown by MOCVD or the ELOG process as a function of fast neutron dose. Reprinted with permission from J. Vac. Sci. Technol. B **28**, 608 (2007). Copyright 2007 American Vacuum Society.

To summarize this section, carrier removal rates in neutron irradiated n-GaN increase with doping and decrease in the sequence MOCVD/ELOG/HVPE. The most prominent traps created were hole traps at 0.6–0.7 eV and electron traps with energy 0.45 eV. The former were associated with disordered regions in GaN and determine the carrier removal rate in undoped films. The latter were attributed to radiation defect complexes with shallow donors. DLTS spectra of neutron irradiated ELOG samples differed from their MOCVD opposite numbers in that the 1 eV N_i-related acceptor state could be clearly seen. However, as with MOCVD, the introduction rates of all traps were several times lower than the electron removal rate, again suggesting the dominant role of DRs in carrier removal. For ELOG material, considerable broadening of x-ray rocking curves for the (0006) symmetric reflection and (11-20) asymmetric reflection occurred as a result of neutron fluence irradiation of $10^{18}\,\mathrm{cm}^{-2}$. This broadening indicates an increased density of extended defects, confirmed by etch pit density (EPD) measurements that show an increase by about $5 \times 10^{7}\,\mathrm{cm}^{-2}$ in the high dislocation density regions and the appearance of new irradiation induced inclined dislocation bands in the low dislocation density wings.

E. Thermal stability of radiation defects in GaN

Annealing studies of defects introduced by light irradiating particles (2 MeV protons, 0.2–2.4 MeV electrons) found that the shallow radiation defects ER1, ER2, and ER3 start annealing at 540 K and the annealing is complete after 620 K.[31] Deeper electron traps ER5 associated with N_i start

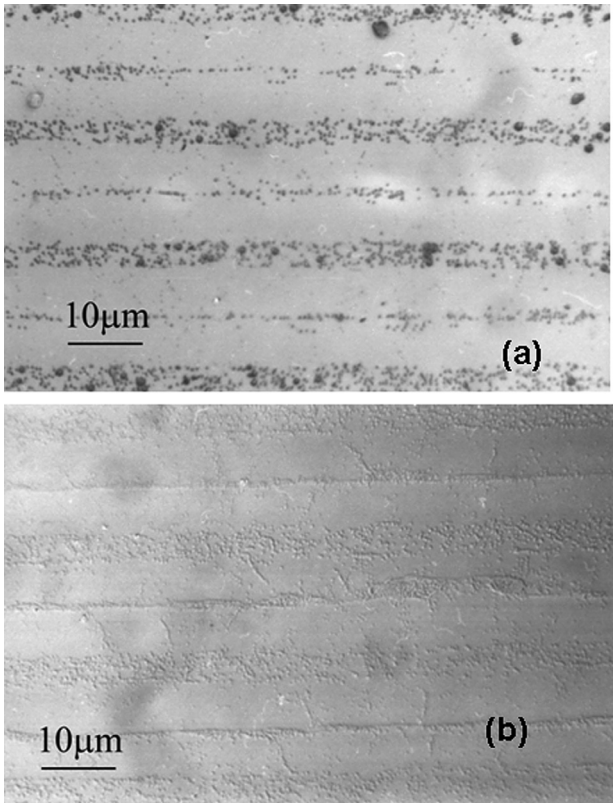

FIG. 8. SEM pictures of ELOG GaN-after neutron irradiation of, inclined dislocation bands propagate into the low-dislocation density ELOG regions. There is also an increased EPD in high-dislocation density areas (increased by $\sim 4 \times 10^7\,\mathrm{cm}^{-2}$ from $5 \times 10^7\,\mathrm{cm}^{-2}$).

annealing also at 540 K, but 660 K was needed for complete removal.[31] Ga_I related deep donors start annealing at room temperature.[28] The V_{Ga} centers responsible for the 0.95 eV PL band were stable up to 500 °C.

In GaN with a high density of radiation defects (high doses of ~100 keV implanted hydrogen or heavier ions, neutron irradiated material), the thermal stability of radiation damage was much higher. After heavy proton implantation, the band-edge luminescence intensity could not be restored to the pre-irradiation value even after annealing at 800 °C.[22] Figure 10 presents the evolution of the sheet resistivity of undoped GaN sample irradiated with fast and thermal neutrons to a fluence of $1.5 \times 10^{17}\,\mathrm{cm}^{-2}$ (the ratio of fast and thermal fluences 1:1).[55] The as-irradiated resistivity decreased at the 150–250 °C stage, increased strongly at the 250–450 °C and then gradually decreased in a very broad stage 500–1000 °C.[55] The first stage corresponds to reconstruction of the ER3 and ER5 acceptors,[31] which explains the decrease in resistivity. The reverse annealing stage at 250–450 °C is most likely due to movement of the N_I, Ga_I centers forming new deep compensating centers. The onset of the third stage of recovery at 500 °C correlates with the V_{Ga} acceptors annealing stage,[28] which explains the decrease of the resistivity. Even after annealing at 800 °C, the preirradiation resistivity was not reached. The Fermi level was pinned at deep centers with activation energy 0.45 eV. The most prominent electron traps were at 0.9 and 1 eV, likely related to the Ga_I donors and the N_I acceptors, but with a high binding energy, possibly trapped within disordered regions. After 1000 °C, annealing the Fermi level was pinned near $E_c - 0.2$ eV and DLTS spectra were dominated by the 0.6 and 0.9 eV traps in high concentration. The total concentrations of the 0.45 eV traps pinning the Fermi level after 800 °C annealing and of the 0.2 eV traps dominant in the 1000 °C annealing are close to each other and equal to the number of donor Ge atoms converted from Ga by interaction with thermal neutrons ($2 \times 10^{16}\,\mathrm{cm}^{-3}$). Hence, these relatively deep traps could be complexes of radiation defects with donor atoms.[55] Even after moderate neutron doses, removal of the disordered regions was incomplete and the initial conductivity was not restored.

For very high neutron fluencies, the resistivity of GaN passes through a maximum related to the onset of hopping conductivity. The activation energy for the temperature dependence of resistivity for doses before the maximum resistivity showed the usual value of 0.9–1 eV. After a fluence corresponding to maximum resistivity, the temperature dependence was weaker and annealing showed a strong reverse

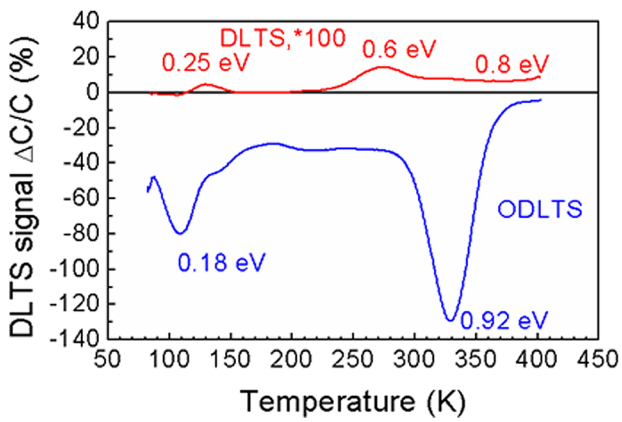

FIG. 9. (Color online) Electron and hole traps in neutron irradiated ELOG regions.

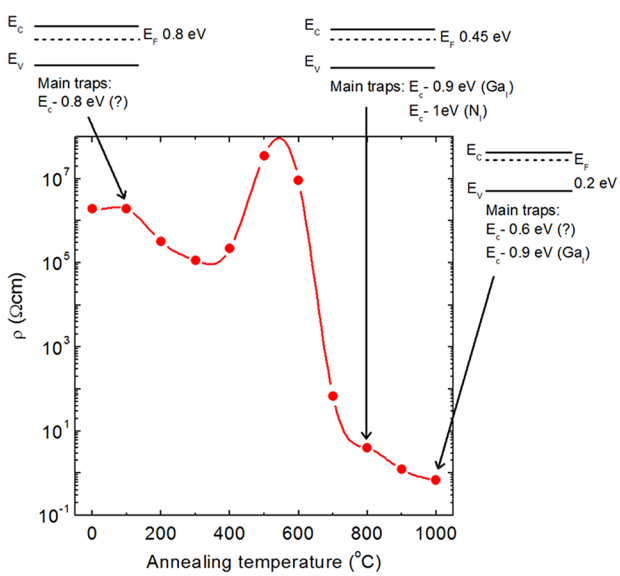

FIG. 10. (Color online) Sheet resistivity as a function of annealing temperature for undoped GaN sample irradiated with fast and thermal neutrons to a fluence of $1.5 \times 10^{17}\,\mathrm{cm}^{-2}$. The position of the Fermi level at different stages is also shown.

annealing stage up to 300 °C where the density of radiation defects decreased and the activation energy returned to the 0.9 eV value. Complete recovery could not be attained even after annealing at 1000 °C.

F. Radiation effects in other III-nitrides

Hall measurements on 150 keV protons and ^{60}Co γ-rays irradiated undoped n-InN films showed that irradiation increased the electron concentration. This difference is closely linked to the difference in the position of the Fermi stabilization level in GaN and InN that determines the difference in the Schottky barrier height between GaN and InN.[72] Increasing the In composition in $In_xGa_{1-x}N$ solid solutions moves the Fermi stabilization level upwards to the conduction band edge. The cross-over point is close to $x = 0.34$, and this composition separates solid solutions in which the electron concentration decreases with irradiation from those in which irradiation increases the electron concentration. Blue LEDs are built on GaN/InGaN quantum well (QW) structures with In mole fraction in the QW close to 0.2, and their behavior should be reasonably close to GaN. For LEDs operating at longer wavelengths, the In composition is higher and care is needed when extrapolating GaN results to these green or red LEDs.

For AlGaN, there are only a few studies of proton and neutron irradiation.[19,102] AlGaN with mole fraction of $x = 0.12$ and free electron concentration of $10^{17}\,cm^{-3}$ irradiated at room temperature and at 300 °C with 2 MeV protons showed carrier removal rates about twice as high as for GaN, decreasing approximately by two times for high temperature irradiation. For undoped n-AlGaN with mole fraction of $x = 0.4$, fast reactor neutron irradiation[65,66] introduced states with activation energy of 0.28 eV at neutron fluences of $10^{15}\,cm^{-2}$ to $2.5 \times 10^{16}\,cm^{-2}$. For higher neutron fluencies, deeper traps with activation energies 0.35 and 1 eV were formed, and the films became semi-insulating with the Fermi level pinned near 0.35 eV from the conduction band edge and sheet resistivity in excess of $10^{14}\,\Omega$/square. From the Schottky barrier height in AlGaN films, 2 eV,[79,80] one would expect the Fermi level to be pinned near $E_c - 2$ eV after high doses of radiation, which accounts for very high resistivity.

The introduction rate for compensating defects for neutron irradiated n-AlGaN was much higher than for undoped n-GaN (about 500 vs $5\,cm^{-1}$) and even higher than in p-GaN [$\sim 100\,cm^{-1}$ (Ref. 2)]. Changes of electrical properties started at a neutron fluence of $10^{15}\,cm^{-2}$, similar to undoped n-GaN,[54] even though the concentration of centers to be compensated was 2 orders of magnitude higher.

The effects of proton implantation were similar to the effects of neutron implantation, but the 100 keV protons start to change electrical properties of AlGaN after a dose of $10^{12}\,cm^{-2}$, two orders of magnitude lower than for undoped n-GaN, despite a much higher donor density in n-AlGaN.[2] The resistivity of the samples rapidly rose with increasing the proton fluence and after irradiation with $10^{14}\,cm^{-2}$ of protons the sheet resistivity was $10^{13}\,\Omega$/square. For p-AlGaN with Al mole fraction of $x = 0.12$, 100 keV proton irradiation caused a decrease in carrier density beginning at a low proton fluence of $10^{12}\,cm^{-3}$. After irradiation with $10^{13}\,cm^{-2}$, the activation energy of the dominant acceptors increased to 0.2 eV while the concentration further decreased. Irradiation with the fluence of $10^{14}\,cm^{-2}$ totally compensated the p-AlGaN film. The observed changes were similar to proton irradiation effects in p-GaN.

G. Effect of radiation species on devices

1. Proton damage

a. HEMTs. The initial work on the effects of proton irradiation on GaN-based heterostructures involved light-emitting diodes, while subsequent work has focused almost exclusively on AlGaN/GaN HEMTs.[103–147] For a proton fluence of $10^{14}/cm^2$ at 1.8 MeV energy, reductions of saturation drain current (I_{DSS}) and transconductance (g_m) in HEMTs from 260 to 100 mA/mm and from 80 to 26 mS/mm, respectively, were reported.[33] Similar proton energy studies at different energies were performed by Hu *et al.*[34] and White *et al.*,[38] which found little degradation and good radiation tolerance of the device channel at fluences up to $10^{14}/cm^2$. For proton irradiation energies of 5 MeV and doses of $2 \times 10^{15}/cm^2$, which is equivalent to roughly 1000 years in low earth orbit, the I_{DSS} of AlGaN/GaN HEMTs was decreased by 43%,[88,95] while at 17 MeV at doses of $2 \times 10^{16}/cm^2$, the reductions were 43% and 29% in I_{DSS} and g_m, respectively.[126,127] A clear effect in these studies is that the proton energy has a strong effect on the amount of damage created in the 2DEG of the HEMT because of differences in nonionizing energy loss.

To simulate the environment in space, Sonia and coworkers[42] also irradiated devices with 2 MeV protons, carbon, oxygen, iron, and krypton ions with fluences ranging from $1 \times 10^9/cm^2$ to $1 \times 10^{13}/cm^2$.[9] The energy dependence of proton-induced degradation was studied by Hu *et al.*;[34] little degradation was observed at 15, 40, and 105 MeV, while 10.6% and 6.1% reductions of drain saturation current and maximum transconductance were obtained at 1.8 MeV energy and fluences of $10^{12}/cm^2$, due to much larger non ionizing energy loss.[58–62] Roy *et al.*[44] studied the radiation response of GaN/AlGaN HEMTs grown by MBE to 1.8-MeV proton fluences. Ammonia-rich HEMTs grown under ammonia-rich conditions were more susceptible to proton-induced degradation, compared to devices grown under Ga-rich or N-rich conditions. Proton irradiation caused positive shifts in pinch-off voltage for all three kinds of devices. N vacancies were suggested to be responsible for an increase of 1/f noise after irradiation.[44,45]

AlGaN/GaN HEMTs show decreases in extrinsic transconductance, drain–source current threshold voltage, and gate current as a result of irradiation with 40 MeV protons at doses equivalent to decades in low-earth orbit. The data are consistent with the protons creating deep electron traps that increase the HEMT channel resistance and decrease mobility.[33,41,89–93] Postirradiation annealing at 300 °C restores ~70% of the initial transconductance (g_m) and drain–source current, (I_{DS}) values in HEMTs receiving proton doses of $5 \times 10^{10}\,cm^{-2}$. The carrier removal rate is about four times higher in InAlN/GaN HEMTs compared to AlGaN/GaN devices, as discussed earlier. Figure 11 shows typical degrees of HEMT device

performance degradation after proton irradiation. Although all the proton-irradiated HEMTs exhibited good pinch-off characteristics, the amount the saturation drain currents were degraded was dependent on the irradiation energy. For the 10 MeV irradiated HEMTs, the reduction of saturation drain current at $V_G = 0$ V was 24%. Much larger saturation drain current reduction, 46%, was observed for the HEMTs irradiated with proton energy at 5 MeV and only 12% drain current reduction exhibited for the HEMTs irradiated with proton energy at 15 MeV. The effect of proton irradiation energies at 5, 10, and 15 MeV at fixed fluence of $5 \times 10^{15}/\text{cm}^2$ has been studied with dc, rf, and power measurements. After irradiation, subthreshold drain leakage current and reverse gate I-V decreased more than one order of magnitude for all cases due to the increase of resistivity of the HEMT channel. The increase in device degradation with decreasing proton energy is due to the increase in linear energy transfer and corresponding increase in nonionizing energy loss with decreasing proton energy in the active region of the HEMTs The proton irradiation creates traps that lower the electric field near the gate and can improve the breakdown characteristic and apparent reliability of the HEMTs, as shown in Fig. 12.

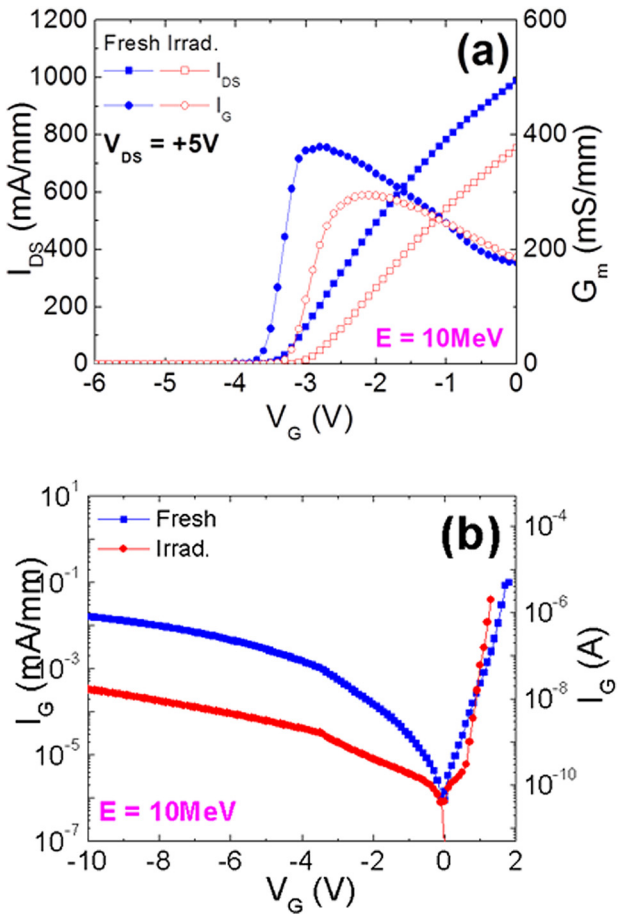

FIG. 11. (Color online) Transfer characteristics from AlGaN/GaN HEMTs before and after irradiation at 10 MeV (a). The extrinsic transconductance, g_m, was reduced and there was a positive shift for the threshold voltage, V_{th}. The reverse and forward gate I-V characteristics of the HEMTs before and after proton irradiation at 10 MeV are shown in (b). Reprinted with permission from J. Vac. Sci. Technol. B **31**, 021205 (2013). Copyright 2013 American Vacuum Society.

For electron irradiation, we found that AlN/GaN HEMTs suffered less degradation in carrier concentration and mobility than their AlGaN/GaN counterparts.[87] This is consistent with the higher average bond strength of the former.

b. LEDs. InGaN MQW LEDs with emission wavelengths from 410 to 525 nm irradiated with 40 MeV protons to doses of 5×10^9–$5 \times 10^{10}\,\text{cm}^{-2}$ (he highest dose is equivalent to more than 100 years in low-earth orbit) showed decreases in electroluminescence (EL) intensity by 15–25% and the reverse breakdown voltage increased by 1–2 V from their control values of ~21–29 V.[111,112] Figure 13 shows typical EL spectra before and after irradiation, in this case for the 445 nm devices. The results were similar for all the wavelengths investigated. The percentage change in breakdown voltage and EL intensity was independent of the initial emission wavelength over the range investigated.

For double heterostructure blue GaN/InGaN LEDs, degradation of the light output started after a dose of 10^{14} neutrons.[103] For proton irradiated AlGaN/GaN QW LEDs, the threshold dose for the onset of degradation was two orders of magnitude higher than for AlGaAs/GaAs QW LEDs ($10^{12}\,\text{cm}^{-2}$ vs $10^{10}\,\text{cm}^{-2}$ for 3 MeV protons). Increasing the proton energy from 3 to 5 MeV increased the dose necessary for the onset of light output degradation, due to a lower energy going into elastic collisions within the active region of devices. Higher proton doses were found necessary for changing the characteristics of proton-irradiated blue GaN/InGaN LEDs.[104] For green GaN/InGaN LEDs,[105] 2 MeV protons produced about 40% light output decrease after a fluence of $1.7 \times 10^{12}\,\text{cm}^{-2}$.

c. Photodetectors. An important characteristic of GaN-based photodetectors is the spectral selectivity, i.e., the ratio of the signal in the UV region and the signal in the visible region. After irradiation with fast reactor neutrons this spectral sensitivity started to change after a fairly large neutron fluence of $10^{15}\,\text{cm}^{-2}$.[106]

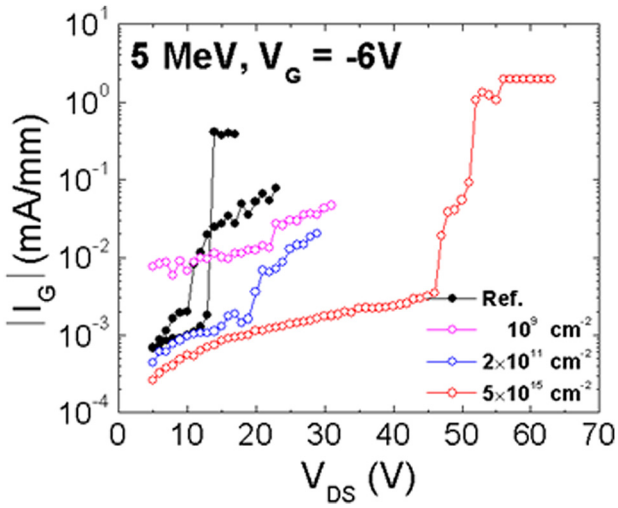

FIG. 12. (Color online) Off-state gate currents as a function of drain voltage for the unirradiated and 10 MeV proton irradiated HEMTs as a function of dose. Reprinted with permission from J. Vac. Sci. Technol. B **31**, 022201 (2013). Copyright 2013 American Vacuum Society.

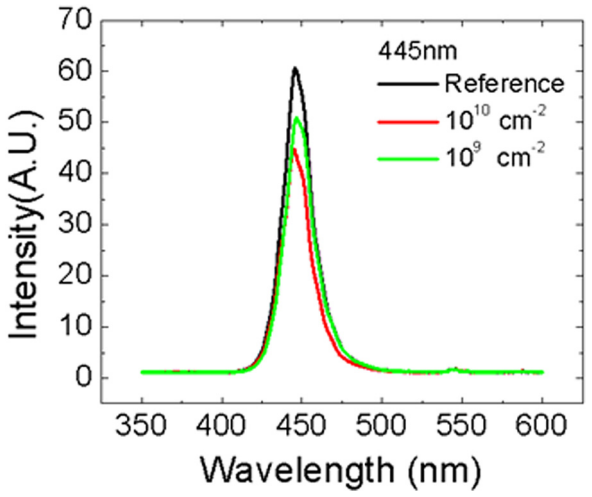

FIG. 13. (Color online) EL spectrum from 445 nm InGaN/GaN LED before and after 40 MeV proton irradiation to doses of 5×10^9 or 5×10^{10} cm^{-2}.

2. Gamma-rays

a. HEMTs. High doses (up to 600 Mrad) of ^{60}Co γ-rays[99] increased reverse breakdown voltage (V_B) by a factor of two, with threshold voltage (V_T) becoming more negative and extrinsic transconductance (g_m) decreased by 20%–30%. The results are consistent with the γ-irradiation causing a decrease in the effective channel doping through introduction of deep electron traps. Table II summarizes the relationship between dose, diffusion length decrease, activation energy increase, and change in capacitance–voltage (C-V) characteristics. An increase in activation energy with gamma-irradiation provides insight into the creation of defect levels in the AlGaN/GaN devices. 0.6 MeV Compton electrons, generated by the interaction of the material with ^{60}Co gamma-photons at average energy of 1.25 MeV, are likely to create donor-type nitrogen vacancy-related defects in III-N layers. These types of defects have been reported after low-energy proton, electron, and gamma irradiation.[6,8,25] Activation energies were seen to increase for HEMTs subjected to the highest gamma-irradiation dose, as shown in Table II.[146] This increase is most likely related to the creation of deep traps due to nitrogen vacancies induced in AlGaN/GaN by gamma-irradiation. The Ga vacancy is an acceptor-like defect and acts as a compensation center, while the nitrogen vacancy acts like a donor. By forming deep traps, these vacancies reduce the carrier concentration, thus increasing the activation energy in the irradiated devices, which leads to an increase of device degradation with gamma-irradiation dose.

TABLE II. Effect of Co-60 gamma ray dose on AlGaN/GaN HEMTs. I_{DS} is drain–source current, G_m is transconductance, and V_{th} is threshold voltage (after Ref. 146).

	Unirradiated	Sample A	Sample B	Sample C
γ-Dose (Gy)	0	300	700	1000
Diffusion length, L (μm)	0.85	0.76	0.52	0.32
Activation energy, ΔEa (meV)	105	125	162	216
ΔI_{DS} (%)	0	−16.5	−37.5	−56.9
Δ Gm (%)	0	−37.9	−54.0	−74.1
Δ Vth	0	0.1	0.44	0.67

b. LEDs. InGaN MQW LEDs with emission wavelengths from 410 to 510 nm were irradiated with ^{60}Co γ-rays with doses in the range of 150–2000 Mrad (Si).[111,112] The forward turn-on voltage was increased by only ~0.1–0.15 V for 500 MRad dose irradiations, while the reverse breakdown voltage was unchanged. The light output intensity for the 410 nm diodes was decreased by 20% after a dose of 150 MRad and 75% after ~2 GRad. The current transport in the LEDs was dominated by generation-recombination (ideality factor ~2) before and after irradiation.

3. Neutron damage

In GaN-based LEDs, changes in quantum efficiency and optical output upon neutron irradiation started at doses of ~10^{14} cm^{-2}, with major contributions coming from changes in the carrier concentration in the active region and a decrease in the minority carriers' diffusion length. Neutron irradiation may cause changes in the I-V characteristics as well as light output.[145] Atomic displacements were responsible for both of the electrical and optical degradation. The increasing value of saturation current after irradiation was attributed to increasing trap concentration. The light output at a bias current of 2.5 mA degraded almost completely (99%) after 1.6 neutron irradiation. Some optical and electrical recovery due to an injection-enhanced annealing effect was observed in our irradiated LEDs. InGaN/GaN multi-quantum well LEDs with emission wavelength of 450 nm were irradiated with neutrons with an average energy of 9.8 MeV and a fixed dose of 5.5×10^{11} cm^{-2}. The forward current of the irradiated LEDs was decreased as a result of the creation of deep trap states by the neutron-induced lattice displacements.[144] However, most of the lattice damage resulting from the collisions with the incoming neutrons was removed by self-annealing at room temperature over a period of 8 days after the irradiation and the current level of devices was recovered to preirradiation levels.

4. Electron damage

Electron irradiation produces strong compensation of the conductivity in GaN/AlGaN multiple quantum wells and introduces interface traps with ionization energies of 100 and 190 meV, in addition to a broad band of interface traps closer to the middle of the bandgap, acceptor traps near $E_c - 1.1$ eV and hole traps near $E_v + 0.9$ eV in the GaN barriers and at the GaN/InGaN interfaces in the QWs. The dose of electrons at which changes occur in the microcathodoluminescence spectra is 10^{15} cm^{-2}, while changes in the electrical properties are observed after doses of 10^{16} cm^{-2} electrons. The most sensitive properties to radiation are luminescence and electroluminescence for which measurable changes occur after irradiation with 10^{15} cm^{-2} electrons. The electrical properties of LEDs start to change after irradiation with 10^{16} cm^{-2} of 10 MeV electrons.[131–134,145] Taking into account the number of displaced atoms, these threshold doses are in reasonable

agreement with the results of neutron and proton irradiation of GaN LEDs. In terms of electron irradiation of HEMTs, doses of $10^{16}\,cm^{-2}$ produce decreases in electron mobility of a factor of 2, while gate current and drain–source current both increase. Low energy electron (<1 MeV) radiation results in an increase in the transistor channel drain current. These increases occur both at low and room temperature.[147] The mechanism causing the increase in drain current is an increase in the carrier concentration in the 2DEG. This is likely due to donor electrons from a nitrogen vacancy in the gallium nitride. The HEMTs begin to anneal immediately after cessation of the irradiation and show almost complete recovery after 72 h.[147] Higher energy (10 MeV) electron irradiation on AlGaN/GaN and AlN/GaN heterojunctions showed the irradiation increases the resistivity of the GaN buffer due to compensation by radiation defects with levels near E_c-1 eV and decreases the mobility of the 2DEG near the AlGaN/GaN (or AlN/GaN) interface.[87] The bulk carrier removal rate in the GaN buffer was the same for both types of structures and similar to carrier removal rates for undoped n-GaN films. In structures with a density of residual donors of $\sim 10^{15}\,cm^{-3}$, irradiation with electron doses of $5\times10^{15}\,cm^{-2}$ rendered the buffer semi-insulating. The 50% degradation of the 2DEG conductivity happened at several times higher doses (close to $3\times10^{16}\,cm^{-2}$ vs $6.5\times10^{15}\,cm^{-2}$) for AlN/GaN than for AlGaN/GaN structures, and shows the AlN is more radiation hard than the AlGaN.[87]

III. SUMMARY AND CONCLUSIONS

The radiation hardness of GaN-based devices is about an order of magnitude higher than for their AlGaAs/GaAs counterparts, a consequence of the higher binding energy in GaN leading to a reduced introduction rate of primary radiation defects. The carrier removal rate in proton irradiated n-GaN is around 10^2–$10^3\,cm^{-1}$ depending on the proton energy and increases for higher donor concentrations mostly because the majority of traps introduced by radiation are shallow. The most prominent deep traps have activation energies of 0.13, 0.16–0.18, 0.2–0.21 eV. Electron irradiation with various energies create 0.16–0.18 eV traps due to N vacancies with ionization energy of 0.07 eV and a high barrier for capture of electrons. Other traps are tentatively ascribed to Ga vacancy complexes with nitrogen interstitials. These defects can be annealed at ~300 °C. For high doses of proton or heavier ions, when aggregates of primary defects can be formed, deeper and more thermally stable electron traps with activation energy 0.75, 0.95 eV were reported. Proton implantation only leads to high sheet resistivities for heavier ions or high proton doses. Neutron irradiation creates disordered regions in which the Fermi level is pinned near $E_c-(0.9–1)$ eV. The Fermi level pinning position is believed to be due to nitrogen-interstitial-related deep acceptors near E_c-1 eV and gallium interstitial-related deep donors near $E_c-(0.8–0.9)$ eV. The latter centers were also observed in GaN samples irradiated with high energy electrons, protons, or heavy ions. The main compensating agents in electron irradiated n-GaN films are the 1.1 eV acceptors often associated with nitrogen interstitials.

Electron irradiation of GaN leads to compensation of n-type conductivity and the carrier removal rate increases substantially with increasing starting donor concentration. For MOCVD samples, the main compensating defect was a 0.15 eV electron trap. Once the Fermi level crossed the level of these traps, two other centers with activation energy of 0.2 and 1 eV were found to contribute to compensation, so that after high doses, the Fermi level in moderately doped samples was pinned near E_c-1 eV. The carrier removal rate in ELOG n-GaN was measurably lower than MOCVD samples with similar doping level.

For neutron irradiation, carrier removal rates are related to the threading dislocation density/distribution, which forms a cellular pattern in MOCVD and in ELOG window regions and randomly distributions in ELOG wing regions and HVPE layers. Differences in dislocation distribution are important for analyzing compensation mechanisms in irradiated material. Major electron traps in neutron irradiated GaN of all types are created at 0.45, 0.85, and 1 eV. The introduction rate for the 0.85 eV traps is well correlated to Ga interstitial donors and for the 1 eV traps to N interstitial acceptors. The latter was close to $0.1\,cm^{-1}$ in MOCVD and ELOG and lower in the HVPE. Neutrons mainly produce damage in the form of disordered regions with the core Fermi level pinned near Ec−(0.8–0.9) eV, surrounded by a space charge region with a high potential barrier for electrons. This effect gives rise to strong persistent conductivity. DR-related carrier removal rates do not vary with the donor doping. The net carrier removal rate is the sum of contributions from DRs and from traps whose introduction rate increases with doping and decreases in the order MOCVD/ELOG/HVPE GaN.

Carrier removal rates in proton irradiated n-GaN are $\sim 10^2$–$10^3\,cm^{-1}$, depending on the proton energy and increase for higher donor concentrations. In p-GaN implanted with 100 keV protons, degradation of luminescent and electric properties starts at doses $\sim 10^{12}\,cm^{-2}$. The threshold dose for observation of decreases in luminescence is more than an order of magnitude lower than in n-GaN due to complex formation between the radiation defects and Mg acceptors. The main deep centers introduced by proton damage in p-GaN have activation energies 0.3, 0.6, and 0.9 eV, while in n-GaN they are 0.2, 0.25, 0.32, 0.45, 0.6, and 0.8 eV. InAlN/GaN HEMTs are very resistant to high energy proton-induced degradation, with <10% degradation in Rs, I_{DSAT}, and g_m for HEMTs irradiated with doses of $2\times10^{13}\,cm^{-2}$, but are less radiation hard than their AlGaN/GaN counterparts.

Radiation effects in GaN can be reasonably well understood based on a picture in which the main radiation defects are due to shallow V_N and deep Ga_i donors and deep V_{Ga} and N_i acceptors. This model places V_N donors near $E_c-0.06$ eV, Ga_i doubly charged donors near $E_c-0.8$ eV, V_{Ga} acceptors near E_v+1 eV, and N_i acceptors near E_c-1 eV. Other prominent defects in n-GaN, relatively shallow ER1-ER3 traps, seem to be complexes of these primary defects, mostly of V_N, with unidentified species, possibly with donors. In p-GaN, there is evidence of defects near $E_c-0.5$ eV that may be Mg complexes with native defects and also of defects of unidentified nature with a level near $E_v+0.3$ eV. The carrier removal rate in GaN for light particles is well accounted for by the introduction of these simple defects. For fast

neutrons, which create large recoil cascades, carrier removal is by disordered regions in which the Fermi level in the core is pinned between the Ga_i donor level and the N_i acceptor level.

Many issues still have to be addressed, including the strong asymmetry in carrier removal rates in n- and p-type materials, the poor understanding of interaction of radiation defects with dislocations and dopants, and the effect of defect transformation upon increasing irradiation temperature and upon annealing. As an example, experiments on low-temperature electron irradiation of GaN suggest that V_{Ga} acceptors are annealed at 500 °C, yet these acceptors can still be detected in neutron irradiated GaN after 1000 °C anneals. Little systematic work has been done on self-annealing rates for different types of radiation exposure. The role of electric fields on migration of radiation-induced defects is not understood, as is the possible role of hydrogen in gate oxides on GaN-based metal-oxide-semiconductor (MOS) structures.

ACKNOWLEDGMENTS

The work at UF was supported by DTRA award HDTRA1-08-10-BRCWMD-BAA. The work at IRM was supported by a grant from Russian Foundation for Basic Research (05-02-08015) and ICTS (3029). The authors thank their collaborators at IRM, A. V. Govorkov N. B. Smirnov, and also Leonid Chernyak at UCF for helpful discussions.

[1]A. M. Kurakin, S. A. Vitusevich, S. V. Danylyuk, H. Hardtdegen, N. Klein, Z. Bougrioua, B. A. Danilchenko, R. V. Konakova, and A. E. Belyaev, J. Appl. Phys. **103**, 083707 (2008).
[2]A. Y. Polaykov, S. J. Pearton, P. Frenzer, F. Ren, L. Liu, and J. Kim, J. Mater. Chem. C **1**, 877 (2013).
[3]H. Nykänen, S. Suihkonen, L. Kilanski, M. Sopanen, and F. Tuomisto, Appl. Phys. Lett. **100**, 122105 (2012).
[4]J. Oila *et al.*, Phys. Rev. B **63**, 045205 (2001).
[5]C. Ionascut-Nedelcsescu, A. Carlone, A. Houdayer, H. J. von Bardelleben, J. L. Cantin, and S. Raymond, IEEE Trans. Nucl. Sci. **49**, 2733 (2002).
[6]G. A. Umana-Membreno, J. M. Dell, T. P. Hessler, B. D. Nener, G. Parish, L. Faraone, and U. K. Mishra, Appl. Phys. Lett. **80**, 4354 (2002).
[7]D. C. Look, G. C. Farlow, P. J. Drevinsky, D. F. Bliss, and J. R. Sizelove, Appl. Phys. Lett. **83**, 3525 (2003).
[8]D. C. Look, D. C. Reynolds, J. W. Hemsky, J. R. Sizelove, R. L. Jones, and R. J. Molnar, Phys. Rev. Lett. **79**, 2273 (1997).
[9]K. Saarinen, T. Suski, I. Grzegory, and D. C. Look, Phys. Rev. B **64**, 233201 (2001).
[10]F. Tuomisto, V. Ranki, D. C. Look, and G. C. Farlow, Phys. Rev. B **76**, 165207 (2007).
[11]F. Tuomisto, D. C. Look, and G. C. Farlow, Physica B **401/402**, 604 (2007).
[12]Q. Yang, H. Feick, and E. R. Weber, Physica B **376/377**, 447 (2006).
[13]L. M. Liang, X. J. Xie, Q. Y. Hao, Y. Tian, and C. C. Liu, Radiat. Meas. **47**, 965 (2012).
[14]X. Fu, T. Ma, C. Zhang, L. Zhang, Z. Zhang, X. Wang, H. Ma, and H. Tu, Nucl. Instrum. Meth. B **286**, 138 (2012).
[15]J. G. Marques, K. Lorenz, N. Franco, and E. Alves, Nucl. Instrum. Meth. B **249**, 358 (2006).
[16]K. Lorenz, J. G. Marques, N. Franco, E. Alves, M. Peres, M. R. Correia, and T. Monteiro, Nucl. Instrum. Meth. B **266**, 2780 (2008).
[17]P. Hacke, T. Detchprohm, K. Hiramatsu, and N. Sawaacki, Appl. Phys. Lett. **63**, 2676 (1993).
[18]S. A. Vitusevich, A. M. Kurakin, R. V. Konakova, A. E. Belyaev, N. Klein, Appl. Surf. Sci. **255**, 784 (2008).
[19]M. Hayes, F. D. Auret, L. Wu, W. E. Meyer, J. M. Nel, and M. J. Legodi, Physica B **340/342**, 421 (2003).
[20]C. Uzan-Saguy, J. Salzman, R. Kalish, V. Richter, U. Tish, S. Zamir, and S. Prawer, Appl. Phys. Lett. **74**, 2441 (1999).
[21]J. Nord, K. Nordlund, and J. Keininen, Phys. Rev. B **68**, 184104 (2003).
[22]T. H. Myers, A. J. Ptak, B. L. VanMil, M. Moldovan, P. J. Treado, M. P. Nelson, J. M. Ribar, and C. T. Zugates, J. Vac. Sci. Technol. B **18**, 2295 (2000).
[23]I. A. Buyanova, M. Wagner, W. M. Chen, B. Monemar, J. L. Lindström, H. Amano, and I. Akasaki, Appl. Phys. Lett. **73**, 2968 (1998).
[24]S. O. Kucheyev, J. S. Williams, and C. Jagadish, Phys. Rev. B **64**, 035202 (2001).
[25]A. Y. Polyakov, N. B. Smirnov, A. V. Govorkov, In-Hwan Lee, Jong Hyeob Baek, N. G. Kolin, V. M. Boiko, D. I. Merkurisov, and S. J. Pearton, J. Electrochem. Soc. **155**, H31 (2008).
[26]D. W. Jenkins, J. D. Dow, and M.-H. Tsai, J. Appl. Phys. **72**, 4130 (1992).
[27]G. A. Umana-Membreno, J. M. Dell, G. Parish, B. N. Nener, L. Faraone, and U. K. Mishra, IEEE Trans. Electron Dev. **50**, 2326 (2003).
[28]K. H. Chow, L. S. Vlasenko, P. Johannesen, C. Bozdog, and G. D. Watkins, Phys. Rev. B **69**, 045207 (2004).
[29]L. Polenta, Z.-Q. Fang, and D. C. Look, Appl. Phys. Lett. **76**, 2086 (2000).
[30]F. D. Auret, S. A. Goodman, F. K. Koschnick, J.-M. Spaeth, B. Beaumont, and P. Gibart, Appl. Phys. Lett. **74**, 407 (1999).
[31]S. A. Goodman, F. D. Auret, F. K. Koschnick, J.-M. Spaeth, B. Beaumont, and P. Gibart, Mater. Sci. Eng. B-Solid **71**, 100 (2000).
[32]M. Senthil Kumar, G. Sonia, D. Kanjilal, R. Dhanasekaran, and J. Kumar, Nucl. Instrum. Meth. B **207**, 308 (2003).
[33]S. J. Cai *et al.*, IEEE Trans. Electron Dev. **47**, 304 (2000).
[34]X. W. Hu *et al.*, IEEE Trans. Nucl. Sci. **50**, 1791 (2003).
[35]J. Neugebauer and C. G. Van de Walle, Phys. Rev. B **50**, 8067 (1994).
[36]P. Boguslawski, E. I. Briggs, and J. Bernholc, Phys. Rev. B **51**, 17255 (1995).
[37]A. P. Karmarkar, B. Jun, D. M. Fleetwood, D. D. Schrimpf, R. A. Weller, B. D. White, L. S. Brillson, and U. K. Mishra, IEEE Trans. Nucl. Sci. **51**, 3801 (2004).
[38]B. D. White, M. Bataiev, S. H. Goss, X. Hu, A. Karmarkar, D. M. Fleetwood, R. D. Schrimpf, W. J. Schaff, and L. J. Brillson, IEEE Trans. Nucl. Sci. **50**, 1934 (2003).
[39]H. Y. Kim, T. Anderson, M. A. Mastron, J. A. Freitas, Jr., S. W. Jang, J. Hite, C. R. Eddy, Jr., and J. Y. Kim, J. Cryst. Growth **326**, 62 (2011).
[40]H. Y. Kim, J. H. Kim, S. P. Yun, K. R. Kim, T. J. Anderson, F. Ren and S. J. Pearton, J. Electrochem. Soc. **155**, H513 (2008).
[41]B. Luo, Jihyun Kim, F. Ren, S. J. Pearton, J. K. Gillespie, and R. C. Fitch, Appl. Phys. Lett. **82**, 1428 (2003).
[42]G. Sonia, E. Richter, F. Brunner, A. Denker, R. Lossy, M. Mai, and F. Lenk, Solid-State Electron. **52**, 1011 (2008).
[43]X. W. Hu *et al.*, IEEE Trans. Nucl. Sci. **51**, 293 (2004).
[44]Tania Roy, En Xia Zhang, Yevgeniy S. Puzyrev, Daniel M. Fleetwood, Ronald D. Schrimp, Bo K. Choi, Anthony B. Hmelo, and Sokrates T. Pantelides, IEEE Trans. Nucl. Sci. **57**, 3060 (2010).
[45]Y. Puzyrev, T. Roy, E. X. Zhang, D. M. Fleetwood, R. D. Schrimpf, and S. T. Pantelides, IEEE Trans. Nucl. Sci. **58**, 2918 (2011).
[46]Byung-Jae Kim, Hong-Yeol Kim, Jihyun Kim, and S. Jang, J. Cryst. Growth **326**, 205 (2011).
[47]S. A. Goodman, F. D. Auret, G. Myburg, M. J. Legodi, P. Gibart, and B. Beaumont, Mater. Sci. Eng. B-Solid **82**, 95 (2001).
[48]T. Ahlgren and E. J. Rauhala, J. Appl. Phys. **90**, 4871 (2001).
[49]J. W. Tringe, A. M. Conway, T. E. Felter, W. J. M. Chan, J. Castelaz, V. Lordi, Y. Xia, C. G. Stevens, and C. Wetzel, IEEE Trans. Nucl. Sci. **55**, 3633 (2008).
[50]R. D. Harris, L. Z. Scheick, J. P. Hoffman, T. Thrivikraman, M. Jenabi, Y. Gim, and T. Miyahira, Proceedings of the 2011 IEEE Radiation Effects Data Workshop (REDW), Atlanta, GA, May 2011 (unpublished).
[51]G. A. Umana-Membreno, J. M. Dell, G. Parish, B. D. Nener, L. Faraone, S. Keller, and U. K. Mishra, J. Appl. Phys. **101**, 054511 (2007).
[52]F. D. Auret, S. A. Goodman, F. K. Koschnick, J.-M. Spaeth, B. Beaumont, and P. Gibart, Appl. Phys. Lett. **73**, 3745 (1998).
[53]F. D. Auret, W. E. Meyer, S. A. Goodman, M. Hayes, M. J. Legodi, B. Beaumont, and P. Gibar, Mater. Sci. Eng.: B **93**, 6 (2002).
[54]A. Y. Polyakov *et al.*, J. Vac. Sci. Technol. B **25**, 436 (2007).
[55]A. Y. Polyakov, N. B. Smirnov, A. V. Govorkov, N. G. Kolin, D. I. Merkurisov, V. M. Boiko, A. V. Korulin, and S. J. Pearton, J. Vac. Sci. Technol. B **28**, 608 (2010).
[56]George D. Watkins, AIP Conf. Proc. **772**, 245 (2005).
[57]P. Johannesen, A. Zakrzewski, L. S. Vlasenko, G. D. Watkins, Akira Usui, Haruo Sunakawa, and Masashi Mizuta, Phys. Rev. B **69**, 045208 (2004).

[58]J. F. Ziegler, J. P. Biersack, and U. Littmark, *The Stopping and Range of Ions in Solids*, 2nd ed. (Pergamon, New York, 1996).
[59]J. R. Srour, C. J. Marshall, and P. W. Marshall, IEEE Trans. Nucl. Sci. **50**, 653 (2003).
[60]J. R. Srour, IEEE Trans. Nucl. Sci. **18**, 359 (1971).
[61]G. C. Messenger and M. S. Ash, *The Effects of Radiation on Electronic Systems*, 2nd ed. (Van Nostrand Reinhold, New York, 1992), pp. 198–203, and references therein.
[62]G. P. Summers, E. A. Burke, P. Shapiro, S. R. Messenger, and R. J. Waters, IEEE Trans. Nucl. Sci. **40**, 1372 (1993).
[63]M. Linde, S. J. Uftring, and G. D. Watkins, Phys. Rev. B **55**, R10177 (1997).
[64]K. H. Chow, G. D. Watkins, A. Usui, and M. Mizuta, Phys. Rev. Lett. **85**, 2761 (2000).
[65]A. Y. Polyakov, N. B. Smirnov, A. V. Govorkov, S. J. Pearton, J. M. Zavada, and R. G. Wilson, J. Appl. Phys. **94**, 3069 (2003).
[66]A. Y. Polyakov *et al.*, J. Vac. Sci. Technol. B **24**, 2256 (2006).
[67]Z.-Q. Fang, J. W. Hemsky, D. C. Look, and M. P. Mack, Appl. Phys. Lett. **72**, 448 (1998).
[68]B. B. Nielsen, J. U. Andersen, and S. J. Pearton, Phys. Rev. Lett. **60**, 321 (1988).
[69]J. W. Johnson *et al.*, Appl. Phys. Lett. **77**, 3230 (2000).
[70]B. R. Gossick, J. Appl. Phys. **30**, 1214 (1959).
[71]A. Y. Polyakov *et al.*, J. Appl. Phys. **100**, 093715 (2006).
[72]W. Walukiewicz, J. Vac. Sci. Technol. B **5**, 1062 (1987).
[73]J. Tersoff, J. Vac. Sci. Technol. B **4**, 1066 (1986).
[74]K. Kuriyama, T. Tokumasu, Jun Takahashi, H. Kondo, and M. Okada, Appl. Phys. Lett. **80**, 3328 (2002).
[75]V. V. Emtsev *et al.*, Physica B: Cond. Mat. **308–310**, 58 (2001).
[76]N. M. Shmidt *et al.*, Phys. Status Solidi B **216**, 533 (1999).
[77]In-Hwan Lee, A. Y. Polyakov, N. B. Smirnov, A. V. Govorkov, A. V. Markov, and S. J. Pearton, Phys. Status Solidi C **3**, 2087 (2006).
[78]A. Y. Polyakov *et al.*, J. Electron. Mater. **36**, 1320 (2007).
[79]A. Y. Polyakov, N. B. Smirnov, A. V. Govorkov, N. V. Pashkova, S. J. Pearton, J. M. Zavada, and R. G. Wilson, J. Vac. Sci. Technol. B **21**, 2500 (2003).
[80]A. Y. Polyakov, N. B. Smirnov, A. V. Govorkov, A. V. Markov, N. G. Kolin, V. M. Boiko, D. I. Merkurisov, and S. J. Pearton, J. Vac. Sci. Technol. B **24**, 1094 (2006).
[81]A. Y. Polyakov, N. B. Smirnov, A. V. Govorkov, K. H. Baik, S. J. Pearton, and J. M. Zavada, J. Vac. Sci. Technol. B **22**, 2291 (2004).
[82]B. H. Rose and C. E. Barnes, J. Appl. Phys. **53**, 1772 (1982).
[83]J. Boch, F. Saigne, R. D. Schrimpf, J. R. Vaille, L. Dusseau, and E. Lorfevre, IEEE Trans. Nucl. Sci. **53**, 3655 (2006).
[84]A. P. Karmarkar, B. D. White, D. Buttari, D. M. Fleetwood, R. D. Schrimpf, R. A. Weller, L. J. Brillson, and U. K. Mishra, IEEE Trans. Nucl. Sci. **52**, 2239 (2005).
[85]F. Gaudreau, P. Fournier, C. Carlone, S. M. Khanna, H. Tang, J. Webb, and A. Houdayer, IEEE Trans. Nucl. Sci. **49**, 2702 (2002).
[86]A. Y. Polyakov, N. B. Smirnov, A. V. Govorkov, A. V. Markov, S. J. Pearton, N. G. Kolin, D. I. Merkurisov, and V. M. Boiko, J. Appl. Phys. **98**, 033529 (2005).
[87]A. Y. Polyakov *et al.*, Appl. Phys. Lett. **93**, 152101 (2008).
[88]X. A. Cao, S. J. Pearton, A. P. Zhang, G. T. Dang, F. Ren, R. J. Shul, L. Zhang, R. Hickman, and J. M. Van Hove, Appl. Phys. Lett. **75**, 2569 (1999).
[89]B. Luo *et al.*, Appl. Phys. Lett. **80**, 604 (2002).
[90]A. Y. Polyakov *et al.*, Physica B: Cond. Mat. **376–377**, 523 (2006).
[91]S. J. Pearton and C. R. Abernathy, Appl. Phys. Lett. **68**, 1793 (1996).
[92]B. D. White *et al.*, IEEE Trans. Nucl. Sci. **49**, 2695 (2002).
[93]B. Luo *et al.*, Appl. Phys. Lett. **79**, 2196 (2001).
[94]A. Kalavagunta, M. Silvestri, M. J. Beck, S. K. Dixit, R. D. Schrimpf, R. A. Reed, D. M. Fleetwood, L. Shen, and U. K. Mishra, IEEE Trans. Nucl. Sci. **56**, 3192 (2009).
[95]H. H. Tan, J. S. Williams, J. Zou, D. J. H. Cockayne, S. J. Pearton, J. C. Zolper, and R. A. Stall, Appl. Phys. Lett. **72**, 1190 (1998).
[96]S. J. Pearton, F. Ren, A. P. Zhang, and K. P. Lee, Materials Sci. Eng. B **30**, 55 (2000).
[97]B. Luo *et al.*, Solid-State Electron. **47**, 1015 (2003).
[98]J. Kim, R. Mehandru, B. Luo, F. Ren, B. P. Gila, A. H. Onstine, C. R. Abernathy, S. J. Pearton, and Y. Irokawa, Appl. Phys. Lett. **81**, 373 (2002).
[99]B. Luo *et al.*, Appl. Phys. Lett. **80**, 1661 (2002).
[100]T. Wosiński, J. Appl. Phys. **65**, 1566 (1989).
[101]Y. Tokuda, Y. Matuoka, K. Yoshida, H. Ueda, O. Ishiguro, N. Soejima, and T. Kachi, Phys. Status Solidi C **4**, 2568 (2007).
[102]A. Y. Polyakov *et al.*, Appl. Phys. Lett. **83**, 2608 (2003).
[103]S. M. Khanna, D. Estan, Alain Houdayer, H. C. Liu, and R. Dudek, IEEE Trans. Nucl. Sci. **51**, 3585 (2004).
[104]F. Gaudraeau, C. Cardone, A. Noudayer, and S. M. Khanna, IEEE Trans. Nucl. Sci. **48**, 1778 (2001).
[105]M. Osinsky, P. Perlin, H. Schone, A. H. Paxtone, and E. W. Taylor, Electron. Lett. **33**, 1252 (1997).
[106]J. Grant, W. Cunningham, A. Blue, V. O'Shea, J. Vaitkus, E. Gaubas, and M. Rahman, Nucl. Instrum. Meth. A **546**, 213 (2005).
[107]J. Grant, R. Bates, W. Cunningham, A. Blue, J. Melone, F. McEwan, J. Vaitkus, E. Gaubas, and V. O'Shea, Nucl. Instrum. Meth. A **576**, 60 (2007).
[108]S. M. Hearne, D. N. Jaimeson, C. Yang, S. Prawer, J. Salzman, and O. Katz, Nucl. Instrum. Meth. B **190**, 873 (2002).
[109]K. K. Allums, M. Hlad, B. P. Gila, C. R. Abernathy, S. J. Pearton, F. Ren, R. Dwivedi, T. N. Fogarty, and R. Wilkins, J. Electron. Mater. **36**, 519 (2007).
[110]S. N. Rashkeev, D. M. Fleetwood, R. D. Schrimpf, and S. T. Pantelides, IEEE Trans. Nucl. Sci. **51**, 3158 (2004).
[111]R. Khanna, K. K. Allums, C. R. Abernathy, S. J. Pearton, J. Kim, F. Ren, R. Dwivedi, T. N. Fogarty, and R. Wilkins, Appl. Phys. Lett. **85**, 3131 (2004).
[112]R. Khanna, S. Y. Han, S. J. Pearton, D. Schoenfeld, W. V. Schoenfeld, and F. Ren, Appl. Phys. Lett. **87**, 212107 (2005).
[113]B. Luo *et al.*, J. Electron. Mater. **31**, 437 (2002).
[114]A. Y. Polyakov, A. V. Govorkov, N. B. Smirnov, N. M. Shmidt, S. J. Pearton, and A. V. Osinsky, Solid-State Electron **47**, 51 (2003).
[115]Francesca Danesin, F. Zanon, S. Gerardin, F. Rampazzo, G. Meneghesso, E. Zanoni, and A. Paccagnella, Microelectron. Rel. **46**, 1750 (2006).
[116]J. C. Zolper, H. H. Tan, J. S. Williams, J. Zou, D. J. H. Cockayne, S. J. Pearton, M. Hagerott Crawford, and R. F. Karlicek, Jr., Appl. Phys. Lett. **70**, 2729 (1997).
[117]S. J. Pearton, C. B. Vartuli, J. C. Zolper, C. Yuan, and R. A. Stall, Appl. Phys. Lett. **67**, 1435 (1995).
[118]J. Kim, R. Mehandru, B. Luo, F. Ren, B. P. Gila, A. H. Onstine, C. R. Abernathy, S. J. Pearton, and Y. Irokawa, Appl. Phys. Lett. **80**, 4555 (2002).
[119]S. J. Pearton, J. C. Zolper, R. J. Shul, and F. Ren, J. Appl. Phys. **86**, 1 (1999).
[120]H. H. Tan, J. S. Williams, J. Zou, D. J. H. Cockayne, S. J. Pearton, and R. A. Stall, Appl. Phys. Lett. **69**, 2364 (1996).
[121]N. Theodoropoulou, A. F. Hebard, M. E. Overberg, C. R. Abernathy, S. J. Pearton, S. N. G. Chu, and R. G. Wilson, Appl. Phys. Lett. **78**, 3475 (2001).
[122]A. Y. Polyakov, I.-H. Lee, N. B. Smirnov, N. G. Kolin, A. V. Korulin, V. M. Boiko, and S. J. Pearton, J. Appl. Phys. **109**, 123703 (2011).
[123]I. Lee, A. Y. Polyakov, N. Smirnov, N. G. Kolin, V. M. Boiko, A. V. Korulin, and S. J. Pearton, J. Electrochem. Soc. **158**, H866 (2011).
[124]J. W. McClory and J. C. Petrosky, IEEE Trans. Nucl. Sci. **54**, 1969 (2007).
[125]A. Kalavagunta, A. Touboul, L. Shen, R. D. Schrimpf, R. A. Reed, D. M. Fleetwood, R. K. Jain, and U. K. Mishra, IEEE Trans. Nucl. Sci. **55**, 2106 (2008).
[126]H.-Y. Kim, J. Kim, L. Liu, C.-F. Lo, F. Ren, and S. J. Pearton, J. Vac. Sci. Technol. B **30**, 012202 (2012).
[127]H.-Y. Kim, C. F. Lo, L. Liu, F. Ren, J. Kim, and S. J. Pearton, Appl. Phys. Lett. **100**, 012107 (2012).
[128]C. F. Lo *et al.*, J. Vac. Sci. Technol. B **29**, 061201 (2011).
[129]J. T. Moran, J. W. McClory, J. C. Petrosky, and G. C. Farlow, IEEE Trans. Nucl. Sci. **56**, 3223 (2009).
[130]S. Kuboyama, A. Maru, H. Shindou, N. Ikeda, T. Hirao, H. Abe, and T. Tamura, IEEE Trans. Nucl. Sci. **58**, 2734 (2011).
[131]C.-F. Lo *et al.*, J. Vac. Sci. Technol. B **30**, 041206 (2012).
[132]C. F. Lo *et al.*, J. Vac. Sci. Technol. B **30**, 031202 (2012).
[133]A. Y. Polyakov *et al.*, J. Vac. Sci. Technol. B **30**, 061207 (2012).
[134]Hong-Yeol Kim, Jihyun Kim, F. Ren, and Soohwan Jang, J. Vac. Sci. Technol. B **28**, 27 (2010).
[135]C. S. Li and S. Subramanian, IEEE Trans. Nucl. Sci **50**, 1998 (2003).
[136]Ching-Wu Wang, Appl. Phys. Lett. **80**, 1568 (2002).
[137]R. X. Wang *et al.*, Appl. Phys. Lett. **87**, 031906 (2005).
[138]K. Kuriyama, M. Ooi, A. Onoue, K. Kushida, M. Okada, and Q. Xu, Appl. Phys. Lett. **88**, 132109 (2006).

[139]V. V. Emtsev, V. Yu. Davydov, V. V. Kozlovskii, G. A. Oganesyan, D. S. Poloskin, A. N. Smirnov, E. A. Tropp, and Yu. G. Morozov, Physica B: Cond. Mat. **401–402**, 315 (2007).
[140]S. Jha, Emil V. Jelenković, M. M. Pejović, G. S. Ristić, M. Pejović, K. Y. Tong, C. Surya, I. Bello, and W. J. Zhang, Microelectron. Eng. **86**, 37 (2009).
[141]Woo-Gwang Jung and Hong-Yeol Kim, Microelectron. Eng. **102**, 60 (2013).
[142]O. Aktas, A. Kuliev, V. Kumar, R. Schwindt, S. Toshkov, D. Costescu, J. Stubbins, and I. Adesida, Solid-State Electron. **48**, 471 (2004).
[143]Dong Uk Lee, Eun Kyu Kim, Byung Cheol Lee, and Dae Kon Oh, Thin Solid Films **516**, 3482 (2008).
[144]H. Ohyama, K. Takakura, M. Hanada, T. Nagano, K. Yoshino, T. Nakashima, S. Kuboyama, E. Simoen, and C. Claeys, Mater. Sci. Eng. B-Solid, **173**, 57 (2010).
[145]B. Luo, J. W. Johnson, D. Schoenfeld, S. J. Pearton, and F. Ren, Solid-State Electron **45**, 1149 (2001).
[146]C. Schwartz *et al.*, Appl. Phys. Lett. **102**, 062102 (2013).
[147]Thomas Jarzen, M.S. thesis, Department of Engineering Physics, Air Force Institute of Technology, 2005.

Steve Pearton received his B.S. degree in Physics from University of Tasmania in 1978 and a Ph.D. degree from University of Tasmania in 1983. He was a postdoc at UC Berkeley prior to joining AT&T Bell Laboratories. He joined the University of Florida in 1994 where he is Distinguished Professor and Alumni Chair in the Department of Materials Science and Engineering.

Steve has been a key figure in developing processing techniques used in compound semiconductor electronics and photonics. At Bell Labs, he developed the use of ion implantation, dry etching, and contact technologies in successive generations of compound semiconductor devices.

At UF, Dr. Pearton has primarily focused on fabrication processes for blue/green/UV GaN-based LEDs, laser diodes, and power electronics. The LEDs are used in displays, automotive lighting, and general illumination when combined with phosphors. His most recent interests have been in developing solid state sensors.

His publications have been cited over 35 000 times in the literature. He is a Fellow of APS, IEEE, AVS, ECS, MRS, and TMS. He received the 2005 Electronics Division Award from ECS, 2007 John Thornton Award from AVS, 2007 J.J. Ebers Award from IEEE, 2011 Adler Award from APS, THE 2011 Gordon Moore Medal from ECS, and the 2011 Bardeen Award from TMS.

Richard A. Deist is a senior undergraduate student in the Department of Materials Science and Engineering at the University of Florida. He currently serves as President of the local Material Advantage Student Program chapter. He has worked extensively with degradation of GaN devices through various university projects and will enter the semiconductor industry to work full time after completing his B.S. degree in May 2013.

Fan Ren is a Distinguished Professor and the ExxonMobil Gator Chemical Engineering Alumni Chair Professor in the Department of Chemical Engineering at the University of Florida. He received a B.S. degree in Applied Chemistry in 1975 from Feng Chia University, a M.S. degree in Chemical Engineering in 1978 from National Cheng Kung University, a M.S. degree in Polymer Science and Engineering, and a Ph.D. degree in Inorganic Chemistry in 1991 from Brooklyn Polytechnic, Brooklyn, NY. He joined UF at 1988. Prior to joining UF, he worked for Bell Laboratories, AT&T at Murray Hill, for 13 years in the areas of GaAs based high electron mobility transistors, heterojunction bipolar transistors, and metal oxide semiconductor field effect transistors. He has published more than 840 journal papers. He is a Fellow of the American vacuum Science, American Physics Society, Electrochemical Society, Institute of Electrical and Electronics Engineers, Materials Research Society, and Society of Photographic Instrumentation Engineers. He has received AVS Albert Nerken Award, NASA Patent Application Initial Award, ECS Electronic and Photonic Division Award, and UF Doctoral Dissertation Advisor/Mentoring Award.

Lu Liu is currently working toward the Ph.D. degree in the department of Chemical Engineering at University of Florida, Gainsville. He received bachelor of engineering at Beijing University of Technology in China. He joined Dr. Fan Ren's group in the Department of Chemical Engineering at University of Florida since December 2009 and received an M.E. degree in December of 2010. His research interests include compound semiconductor materials and devices, especially on the studies of reliability and radiation effects of gallium nitride (GaN) based high electron mobility transistors (HEMTs). Since 2010, Lu Liu has published over 50 journal and proceeding papers. He is also a student member of the Electron Devices Society, Reliability Society and Power Electronics Society of the Institute of Electrical and Electronics Engineers (IEEE), Electrochemistry Society (ECS), and America Vacuum Society (AVS).

Alexander Y. Polyakov was born in Moscow, Russia, graduated from Semiconductor Materials Science Department of Moscow Institute of steel and Alloys (MISIS) in 1973. His M.S. thesis was devoted to studies of close range ordering in Ge-Si solid solutions. He got his Ph.D. degree from MISIS in 1982 for studies of radiation effects in InSb photodetectors. Since that time he was employed by the Institute of Rare Metals (Giredmet) in Moscow doing research on various aspects of materials science of III-V and II-VI semiconductors. In 1990–1992, 1995–1997, and 2003–2005, he worked as a visiting researcher at ECE Department and MSE Department of Carnegie Mellon University doing research on MBE growth and characterization of AlGaInSb quarternaries (with Professor A.G. Milnes), on MOCVD growth and characterization of GaN, AlGaN, GaBN, AlBN (with Professor M. Skowronsky and Professor D. Greve), on HCVD growth and characterization of SiC (Professor M. Skowronsky). In 2010–2011, he worked as a visiting professor at Chonbuk National University (Korea, with Professor In-Hwan Lee) doing research on localized surface plasmons in GaN LEDs, on nonpolar AlGaN/GaN HEMTs, and GaN/InGaN MQW LEDs. He is an author or co-author of more than 300 papers, 2 monographs, multiple invited chapters in books on III-V semiconductors, and multiple review articles. His areas of expertise are deep traps in compound semiconductors, properties of heterojunctions and QWs, hydrogen passivation effects, and radiation defects studies.

Jihyun Kim is an associate professor in the Department of Chemical and Biological Engineering at Korea University. He received his B.S. and Ph.D. degrees from Seoul National University (2000) and the University of Florida (2004), respectively. He did his internship at Bell Laboratories in 2003. Then, he joined US Naval Research Laboratory in Washington, DC in 2004 to work on the optical characterizations of Wide-bandgap Semiconductors (SiC and III-nitrides). In 2006, he joined the faculty of the Department of Chemical and Biological Engineering at Korea University as an assistant professor. He has published over 120 journal papers in the area of wide-bandgap semiconductor processing and characterizations and holds 11 patents.